AMERICAN SOCIETY FOR MICROBIOLOGY | Molecular and Cellular Biology®

RESEARCH ARTICLE

# EHD1 and RUSC2 Control Basal Epidermal Growth Factor Receptor Cell Surface Expression and Recycling

**Eric C. Tom,[a,b] Insha Mushtaq,[a,c] Bhopal C. Mohapatra,[a,d] Haitao Luan,[a] Aaqib M. Bhat,[a,d] Neha Zutshi,[a,c] Sukanya Chakraborty,[a,d] Namista Islam,[a,d] Priyanka Arya,[a,d*] Timothy A. Bielecki,[a] Fany M. Iseka,[a,d*] Sohinee Bhattacharyya,[a,c] Luke R. Cypher,[a*] Benjamin T. Goetz,[a] Simarjeet K. Negi,[d*] Matthew D. Storck,[a] Sandeep Rana,[a] Angelika Barnekow,[f] Pankaj K. Singh,[a,b,c,d,e] Guoguang Ying,[g] Chittibabu Guda,[d,e] Amarnath Natarajan,[a,e] Vimla Band,[a,d,e] Hamid Band[a,b,c,d,e]**

[a]Eppley Institute for Research in Cancer and Allied Diseases, University of Nebraska Medical Center, Omaha, Nebraska, USA
[b]Department of Biochemistry and Molecular Biology, University of Nebraska Medical Center, Omaha, Nebraska, USA
[c]Department of Pathology and Microbiology, University of Nebraska Medical Center, Omaha, Nebraska, USA
[d]Department of Genetics, Cell Biology and Anatomy, College of Medicine, University of Nebraska Medical Center, Omaha, Nebraska, USA
[e]Fred and Pamela Buffett Cancer Center, University of Nebraska Medical Center, Omaha, Nebraska, USA
[f]Department of Experimental Tumorbiology, Westfälische Wilhelms University Muenster, Muenster, Germany
[g]Laboratory of Cancer Cell Biology, National Clinical Research Center for Cancer, Tianjin Key Laboratory of Cancer Prevention and Therapy, Tianjin Medical University Cancer Institute and Hospital, Tianjin, China

Eric C. Tom and Insha Mushtaq are co-first authors. Eric C. Tom initiated the project and performed the majority of the studies. Insha Mushtaq completed the project and carried out studies for manuscript revision.

**ABSTRACT** Epidermal growth factor receptor (EGFR) is a prototype receptor tyrosine kinase and an oncoprotein in many solid tumors. Cell surface display of EGFR is essential for cellular responses to its ligands. While postactivation endocytic trafficking of EGFR has been well elucidated, little is known about mechanisms of basal/preactivation surface display of EGFR. Here, we identify a novel role of the endocytic regulator EHD1 and a potential EHD1 partner, RUSC2, in cell surface display of EGFR. EHD1 and RUSC2 colocalize with EGFR in vesicular/tubular structures and at the Golgi compartment. Inducible EHD1 knockdown reduced the cell surface EGFR expression with accumulation at the Golgi compartment, a phenotype rescued by exogenous EHD1. RUSC2 knockdown phenocopied the EHD1 depletion effects. EHD1 or RUSC2 depletion impaired the EGF-induced cell proliferation, demonstrating that the novel, EHD1- and RUSC2-dependent transport of unstimulated EGFR from the Golgi compartment to the cell surface that we describe is functionally important, with implications for physiologic and oncogenic roles of EGFR and targeted cancer therapies.

**KEYWORDS** EGFR, EHD1, endocytic trafficking, cell proliferation

The plasma membrane of metazoan cells provides a fundamental interface for cell-to-cell and cell-to-environment communication. Understanding how the cell surface levels of receptors that recognize and communicate changes in a cell's environment into alterations of a cell's biochemical machinery are regulated is therefore of fundamental interest in cell biology. Receptor tyrosine kinases (RTKs) are a particularly important class of surface receptors as they provide a pervasive mechanism of signal transduction in higher eukaryotes (1). The surface expression of RTKs and their compartmentalization are key determinants of the spatial-temporal signaling output of their ligand-induced activation and dictate the magnitude, duration, and potentially the type of physiological responses (2, 3). Aberrant overexpression or mutational activation of RTKs is a widespread mechanism to drive oncogenesis, and many targeted therapeutics are directed at RTKs or their signaling cascades (4).

**Citation** Tom EC, Mushtaq I, Mohapatra BC, Luan H, Bhat AM, Zutshi N, Chakraborty S, Islam N, Arya P, Bielecki TA, Iseka FM, Bhattacharyya S, Cypher LR, Goetz BT, Negi SK, Storck MD, Rana S, Barnekow A, Singh PK, Ying G, Guda C, Natarajan A, Band V, Band H. 2020. EHD1 and RUSC2 control basal epidermal growth factor receptor cell surface expression and recycling. Mol Cell Biol 40:e00434-19. https://doi.org/10.1128/MCB.00434-19.



Address correspondence to Vimla Band, vband@unmc.edu, or Hamid Band, hband@unmc.edu.

* Present address: Priyanka Arya, Advocate Health Care, Rosemont, Illinois, USA; Fany M. Iseka, Department of Pathology and Laboratory Medicine, University of Pennsylvania School of Medicine, Philadelphia, Pennsylvania, USA; Luke R. Cypher, Department of Pathology, Medical University of South Carolina College of Medicine, Charleston, South Carolina, USA; Simarjeet K. Negi, National Cancer Institute National Institutes of Health, Rockville, Maryland, USA.

**Received** 11 September 2019
**Returned for modification** 26 September 2019
**Accepted** 26 December 2019
**Accepted manuscript posted online** 13 January 2020
**Published** 16 March 2020

Epidermal growth factor receptor (EGFR), the founding member of the ErbB receptor family, is a prototype RTK with critical roles in development and maintenance of epithelial and other tissues by generating cell proliferation, survival, differentiation, and migration cues in response to members of the EGF family of growth factors (5). Activation of ErbB receptors is linked to the initiation and progression of human cancers, and the levels of their expression are often significantly elevated in many solid tumors (e.g., breast, colon, ovary, pancreas, and glial) (6–8). EGFR expression is a feature of the basal-like breast cancer subtype, which has an especially poor prognosis (9).

Given key physiological and oncogenic roles of EGFR, many previous investigations have elucidated mechanisms that control the endocytic trafficking of ligand-activated EGFR, including the ligand-induced activation of both clathrin-dependent and clathrin-independent endocytosis and differential transport into lysosomal degradation or endocytic recycling based on the nature of activating ligands and their concentrations (10, 11). Accordingly, impaired endocytosis or diminished lysosomal targeting of EGFR or other RTKs has emerged as a mechanism by which RTKs become oncogenic (12–14). The Cbl family of ubiquitin ligases are key to sorting EGFR and other RTKs for lysosomal degradation and attenuation of their signaling (15). Indeed, mutations in Cbl are now known to drive a small subset of myeloid leukemias (16).

In contrast to the mechanisms of ligand-activated EGFR trafficking through the endocytic pathway, mechanisms that help maintain the optimal activation-ready pool of cell surface EGFR prior to ligand binding are much less clear. In the absence of a ligand, EGFR is constitutively internalized at a slow rate and thought to primarily recycle (17). It is estimated that 2 to 3% of unoccupied EGFRs on typical cultured cells are endocytosed per minute and rapidly recycle to the plasma membrane (18, 19). However, few studies have sought to characterize mechanisms that regulate the cell surface levels, endocytosis, or recycling of EGFR or other RTKs under their basal unstimulated state. A recent study of EGFR on mouse embryonic fibroblasts (MEFs) in which the Arp2/3-activator Wiskott-Aldrich syndrome protein and Scar homologue (WASH) was deleted showed reduced basal EGFR levels at the cell surface, apparently due to increased diversion to the lysosome (20). As WASH serves as an actin-nucleating component of the retromer complex, which is involved in retrograde trafficking of receptors from endosomes to the Golgi compartment (21), this study suggested that retrograde transport into the Golgi compartment may in part regulate the cell surface EGFR levels. Notably, sorting nexins 1 and 2, which are included in the retromer complex, have been primarily characterized as regulators of ligand-induced lysosomal traffic of EGFR and other RTKs (22).

Members of the highly homologous and evolutionarily conserved EPS-15 homology (EH) domain-containing (EHD) protein family localize to tubular and vesicular endocytic compartments and regulate trafficking of a number of nonsignaling receptors, such as transferrin receptor, major histocompatibility complex class I (MHC-I), and $\beta$1 integrin, from the endocytic recycling compartment (ERC) to the cell surface (23–25). A role for EHD proteins has also emerged in retrograde trafficking from endosomes to the Golgi compartment. Expression of a dominant negative EHD1 mutant in Chinese hamster ovary cells was shown to slow down the transport from the cell surface to the Golgi compartment of TGN38, a marker of endocytic recycling compartment-mediated retrograde transport, but not that of furin, which is transported through the lysosomal route (26). EHD1 binds to vacuolar protein sorting 26 (Vps26) and Vps35, members of the retromer cargo recognition complex, and these interactions were shown to be required for endosome-to-Golgi retrieval of the cation-independent mannose-6-phosphate receptor (27). EHD3 was shown to be necessary for the maintenance of Golgi morphology and transport of endocytosed Shiga toxin B to this organelle (28).

Previous studies in primary neurons and a neuronal cell line showed that neurotrophin activation of TrkA, an RTK, transcriptionally upregulated the expression of EHD4 (referred to as "pincher" in that study) and that EHD4 in turn facilitated the retrograde trafficking of activated TrkA from dendrites to the neuronal body, thereby promoting neurotrophin signaling through this receptor (29). Notably, ligand-induced retrograde

trafficking of EGFR in the same system was not dependent on EHD4 (30). EHD1 and its binding partner SNAP29 were found to be associated with insulin-like growth factor (IGF)-activated IGF1 receptor (IGF1R) and to colocalize with it in endosomes, with EHD1 overexpression resulting in reduced IGF1-induced signaling (31). One study reported that EHD2 interacts with glucose transporter 4 (GLUT4) and colocalizes with it on endosomes, with intracellular application of anti-EHD2 antibody or a peptide blocker, resulting in reduced GLUT4 exocytosis to the plasma membrane (32). Another study found no role of EHD2 in GLUT4 localization in the perinuclear region or in its insulin-stimulated surface transport; instead, the study showed that EHD1 and its interacting partner EHBP1 regulate the perinuclear localization of GLUT4 and its surface transport upon insulin stimulation (33). Neither study reported any role of EHD proteins in the trafficking of insulin receptor. Notably, we observed reduced expression of vascular endothelial growth factor receptor 2 (VEGFR2, an RTK) in glomerular endothelial cells of EHD3/EHD4 (EHD3/4) knockout (KO) mice, which display thrombotic renal glomerular angiopathy, suggesting a potential role of EHD3/4 in VEGFR2 trafficking (34).

More recently, mouse models of EHD deficiency or cells derived from these animals have provided support for the role of EHD proteins in regulating the surface display of non-RTK receptors. EHD1-null MEFs or MEFs with small interfering RNA (siRNA)-mediated EHD1 depletion were reported to show reduced overall but increased activated $\beta$1 integrin levels at the cell surface, with impaired focal adhesion disassembly and cell migration reflecting aberrant $\beta$1 integrin trafficking (24). We have shown that EHD family members participate in cell surface trafficking of sodium/calcium ($Ca^{2+}$) exchanger (35, 36), L-type $Ca^{2+}$ channel type 1.2 (37), and voltage-gated T-type $Ca^{2+}$ channels CaV3.1 and CaV3.2 (38) in cardiomyocytes and of the ferlin protein Fer1L1 (39, 40) in skeletal muscle cells. These findings raised the possibility that EHD proteins also function in the surface expression of RTKs. Recently, using wild-type and EHD1-null bone marrow-derived macrophages, we found that EHD1 is required for the basal surface expression of the RTK colony-stimulating factor 1 (CSF1) receptor (41). In previous work investigating the subcellular organelles where constitutively active non-small cell lung cancer (NSCLC)-associated EGFR mutants traffic, we observed the colocalization of EHD1 and mutant EGFR in the endocytic recycling compartment (42). Expression of EHD1 in NSCLC patients was found to correlate with high levels of EGFR and the Rab11 interactor RAB11-FIP3 as well as with shorter survival (43, 44). A similar analysis in breast cancer showed a positive correlation between EHD1 and RAB11-FIP3 expression, and the expression of these markers correlated with phospho-EGFR levels in tumors; EHD1-positive ($EHD1^+$) patients had a shorter overall and disease-free survival, and a patient status of $EHD1^+$ plus phospho-$EGFR^+$ was even more predictive of shorter survival (45). EHD1 and EGFR expression levels were also reported to be increased in human papillary thyroid cancer, and levels of EHD1 protein were significantly associated with tumor size, lymph node metastasis, and EGFR expression (46). EHD1 levels in NSCLC also showed a negative correlation with sensitivity to EGFR-targeted kinase inhibitor therapy (47). How EHD1 may be involved in regulating EGFR biology, however, is not known. A recent study suggested that EHD3 may function in targeting the ligand-stimulated EGFR to lysosomal degradation by diverting it from endocytic recycling (48), consistent with EHD3 deletion in glioblastoma (49), although doxycycline (Dox)-inducible EHD3 expression in EHD3-deleted glioblastoma cell lines increased the basal levels of EGFR (48). Studies presented here reveal a novel role of EHD1, in conjunction with a new potential interacting partner, RUN and SH3 domain-containing protein 2 (RUSC2) (50), in the transport of EGFR from the Golgi compartment to the surface.

RUSC2/iporin contains a RUN domain (named based on its presence in RPIP8, UNC-14, and NESCA proteins) that interacts with Rab1 and Rab35 small GTPases (51, 52). RUSC2 has also been reported to interact with the Golgi protein GM130 and has been proposed as a potential regulator of endosomal targeting of vesicles derived from the endoplasmic reticulum (ER) (50). We noted RUSC2 as an uncharacterized protein identified in an EGFR-associated protein complex isolated from cells in the absence of

ligand stimulation (53). Here, we show that EHD1 and RUSC2 show an overlapping subcellular localization and function as positive regulators of the transport of unstimulated EGFR from the Golgi compartment to the cell surface to help maintain an activation-ready cell surface pool of EGFR on the plasma membrane.

## RESULTS

While a substantial body of literature has focused on mechanisms involved in the trafficking itinerary of ligand-activated EGFR and the impact of receptor activation on subsequent signaling and biological outcomes (10, 11, 54), relatively little is known about the regulatory mechanisms that control the trafficking of unstimulated EGFR to ensure a cell-optimal display of activation-ready EGFR at the cell surface. Given the role of EHD family proteins, in particular EHD1, in the surface expression of non-RTK receptors and our previous observation that EHD1 colocalized with the oncogenic mutant EGFR in the endocytic recycling compartment (42), we examined the role of EHD1 in the surface display of EGFR under unstimulated conditions.

**EHD1 KD reduces the total EGFR levels on 16A5 MECs both under steady-state and ligand-free culture.** 16A5 is a nontumorigenic, human papillomavirus 16 (HPV16) E6/E7-immortalized and EGF-dependent human mammary epithelial cell (MEC) line (55) that displays the expected ligand-induced EGFR degradation kinetics (56–60) (Fig. 1A). 16A5 as well as other cell lines, including the triple-negative breast cancer cell line MDA-MB-231 and the pancreatic cancer cell line S2013 used in this work, express EHD1 as well as other EHD proteins (Fig. 1B); mouse embryonic fibroblasts (MEFs), the other cell type we use, are known to express EHD1 and other family members as well, and EHD1 was critical for primary cilium biogenesis in these cells (61). To examine the impact of EHD1 knockdown (KD) on total EGFR levels, we transduced 16A5 cells with doxycycline (Dox)-inducible lentiviral constructs expressing a control nontargeting short hairpin RNA (shRNA) or an shRNA directed against the 3′ untranslated region (UTR) of EHD1. Cells were kept at steady state in EGF-containing DFCI medium (55) and pretreated with Dox for 3 days to induce sufficient EHD1 KD; cells were then replated in Dox, and lysates were prepared over a 5-day time course and analyzed by Western blotting. Under conditions of EHD1 KD, we observed a steady reduction in total EGFR levels over the course of the experiment (Fig. 1C and D). We then sought to determine whether the observed depletion was dependent on ligand stimulation. Absence of EGF is known to lead to accumulation of EGFR in an inactive state (unphosphorylated) and increased localization at the cell surface as the receptor is not subject to ligand-induced lysosomal degradation (62). To determine the impact of EHD1 KD under basal ligand-free conditions, we used the 16A5 cell lines engineered with two distinct shRNA sequences targeting EHD1 or a nontargeting control. The cells were pretreated with Dox for 3 days under steady-state conditions and replated in Dox. After 24 h, cells were subjected to EGF deprivation in conjunction with continued Dox treatment and assayed at the indicated time points (0, 6, 12, and 24 h). Total EGFR levels measured by Western blotting were reduced in EHD1 KD cells relative to levels in controls, as seen in representative blots and quantified data from three independent experiments (Fig. 1E and F). To further validate this finding, we carried out overnight transfection of 16A5 cells with distinct siRNAs directed against EHD1 in low-serum Opti-MEM and allowed the cells to recover in regular culture medium for 24 h. Cells were then switched to EGF-free medium for 24 h, followed by Western blotting of lysates. We observed a moderate depletion of total EGFR levels in EHD1 KD cells relative to levels in controls (Fig. 1G and H).

Although the use of multiple distinct siRNAs or shRNAs and analysis of knockout MEFs (see below) make any off-target effects of the knockdown approach remote, we carried out rescue analyses to rigorously validate our findings. We generated 16A5 cell lines that coexpress an exogenous Dox-inducible EHD1-green fluorescent protein (GFP) fusion construct lacking the 3′ UTR of EHD1, and thus resistant to the EHD1 3′ UTR-targeted shRNAs, together with the EHD1-directed shRNA or a control shRNA. Cells were pretreated with Dox for 2 days prior to initiating serum and EGF deprivation. Cells

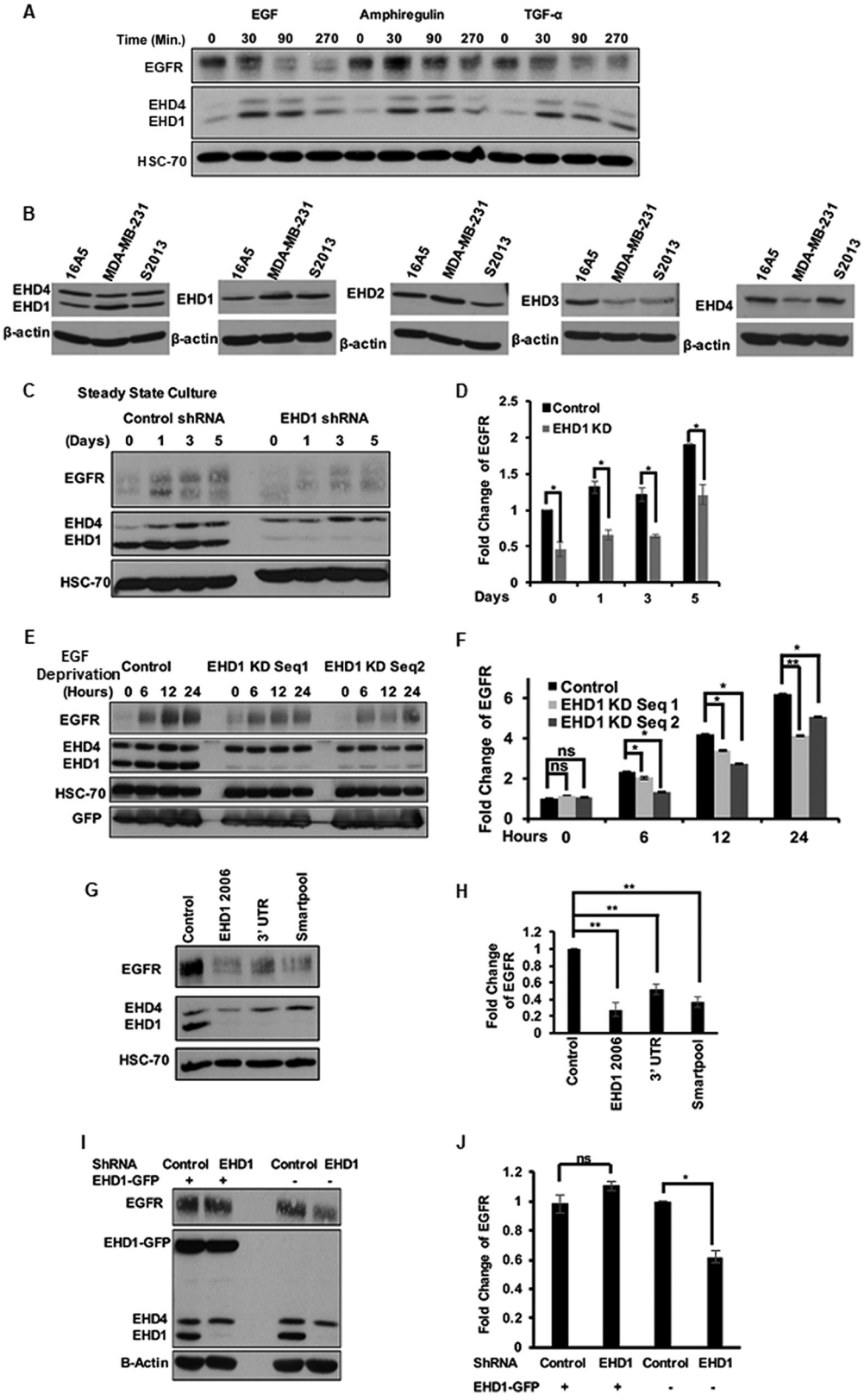


**FIG 1** EHD1 knockdown in 16A5 mammary epithelial cells leads to reduced total and cell surface EGFR levels. (A) 16A5 cells respond to EGF ligands. The 16A5 immortalized human mammary epithelial cells were deprived of serum and EGF for 48 h and then treated with 2 nM EGF, amphiregulin, or transforming growth factor alpha (TGF-$\alpha$) for the indicated times. Cell lysates were immunoblotted for EGFR, EHD1/4, and HSC-70 (loading control). Note that all ligands reduce

(Continued on next page)

coexpressing the shRNA-resistant EHD1-GFP together with EHD1-specific shRNA displayed total EGFR levels comparable to those in the EHD1-GFP-expressing cell line coexpressing a control shRNA. In contrast, cells transduced with only a control empty vector in conjunction with the EHD1 shRNA displayed reduced EGFR levels (Fig. 1I and J).

**EHD1 knockdown reduces the cell surface EGFR levels on 16A5 mammary epithelial cells under ligand-free culture.** To assess if EHD1 KD impacted the surface EGFR expression, we examined the cell surface levels of EGFR in control and EHD1 KD 16A5 cells using fluorescence-activated cell sorter (FACS) analysis. Correlating with the depletion of total levels of EGFR, the surface EGFR levels were reduced in EHD1 KD cells relative to levels of the controls (Fig. 2A and B). To assess if non-RTK receptor expression is impacted by EHD1 depletion under the conditions where we observe an impairment of EGFR expression, we carried out FACS analysis of MHC class I (MHC-I) expression in control and EHD1 KD 16A5 cells cultured under conditions similar to those used for EGFR analyses (growth in serum- and EGF-deprived medium). Previous studies in which MHC-I internalized from the cell surface was tracked showed that EHD1 is required for exit of MHC-I from the endocytic recycling compartment back to the cell surface (Fig. 2C and D). However, MHC-I cell surface levels were comparable in EHD1 KD and control cells.

**EHD1 knockout or knockdown in other cell systems reduces the total EGFR levels under ligand-free culture.** To determine whether the reduction in total EGFR levels upon EHD1 depletion could be seen in cell types other than the 16A5 MECs, we used an isogenic pair of EHD1-floxed and EHD1-null mouse embryonic fibroblasts (MEFs) (61). MEFs were plated in regular medium (without supplemental EGF) for 2 days, followed by treatment with 2 nM EGF for 4.5 h to promote EGFR degradation, and the cells were then subjected to serum and EGF deprivation. As in 16A5 cells, we observed a diminished capacity for the recovery of total EGFR levels over time in EHD1-null MEFs compared to levels in control MEFs although the impact was modest (Fig. 3A and B). Moderate EHD1 dependence of the accumulation of EGFR after serum and EGF deprivation was also seen when we compared control shRNA and EHD1 shRNA-expressing versions of a triple-negative breast cancer cell line, MDA-MB-231 (Fig. 3C and D), or a pancreatic adenocarcinoma cell line, S2013 (Fig. 3E).

Based on these findings, we conclude that EHD1 plays a key positive role in the maintenance of total and cell surface levels of EGFR under basal, ligand-unstimulated conditions.

**FIG 1** Legend (Continued)
the EGFR levels at late time points, more pronounced with EGF. (B) Relative expression of all four EHD proteins in cell lines examined in this work. Whole-cell lysates of the 16A5 MEC line, MDA-MB-231 breast cancer cell line, and S2013 pancreatic cancer cell line were immunoblotted with anti-EHD1/4, anti-EHD1, anti-EHD2, anti-EHD3, or anti-EHD4 antibodies as well as $\beta$-actin (loading control). (C) EHD1 knockdown reduces EGFR levels in 16A5 cells under steady-state culture. 16A5 cells stably transduced with Dox-inducible nontargeting or EHD1-targeted shRNA (EHD1 shRNA without specification indicates sequence 1 [Seq. 1] directed at the 3′ region and refers to clone V2IHSPGG_388688; in other panels where Seq. 1 and 2 are specified, Seq. 2 refers to clone V2IHSPGG_908952) were treated with Dox over 5 days. Cells were maintained in regular medium (steady state), and lysates were collected at the indicated time points and blotted for EGFR and HSC-70 (loading control). (D) Densitometric quantification of EGFR results from the experiment shown in panel B ($n = 3$), normalized to the level for the HSC-70 control. *, $P < 0.05$. (E) EHD1 knockdown reduces EGFR levels in 16A5 cells under ligand-free culture. Stably transduced 16A5 cells expressing Dox-inducible nontargeting or EHD1-targeted shRNA sequences were cultured with Dox for 3 days before serum and EGF deprivation for the indicated times, and lysates were blotted for EGFR and HSC-70 (loading control). (F) Densitometric quantification of EGFR results from the experiment shown in panel D normalized to the level of HSC-70 ($n = 3$). *, $P < 0.05$; **, $P < 0.02$; ns, not significant. (G) Reduction in EGFR levels in 16A5 cells after transient siRNA knockdown of EHD1. 16A5 cells were transiently transfected with the indicated control or EHD1-targeted siRNA oligonucleotides. Lysates of cells deprived of EGF and serum for 24 h were blotted for EGFR, EHD1/4, and HSC-70. (H) Quantification of results presented in panel F normalized to the level for HSC-70 ($n = 3$). *, $P < 0.05$; **, $P < 0.02$. (I and J) Rescue of the effect of EHD1 knockdown on EGFR levels by exogenous, shRNA-resistant EHD1. 16A5 cells stably transduced with nontargeting control or EHD1 3′-UTR-targeted shRNA (Seq. 1) were cotransduced with either Dox-inducible EHD1-GFP or empty vector. Cells pretreated with Dox were EGF and serum starved for 24 h, and lysates were blotted for EGFR and $\beta$-actin (loading control). Densitometric quantification of EGFR levels presented in panel H were normalized to the level for $\beta$-actin ($n = 3$). *, $P < 0.05$, **, $P < 0.02$; ns, not significant.

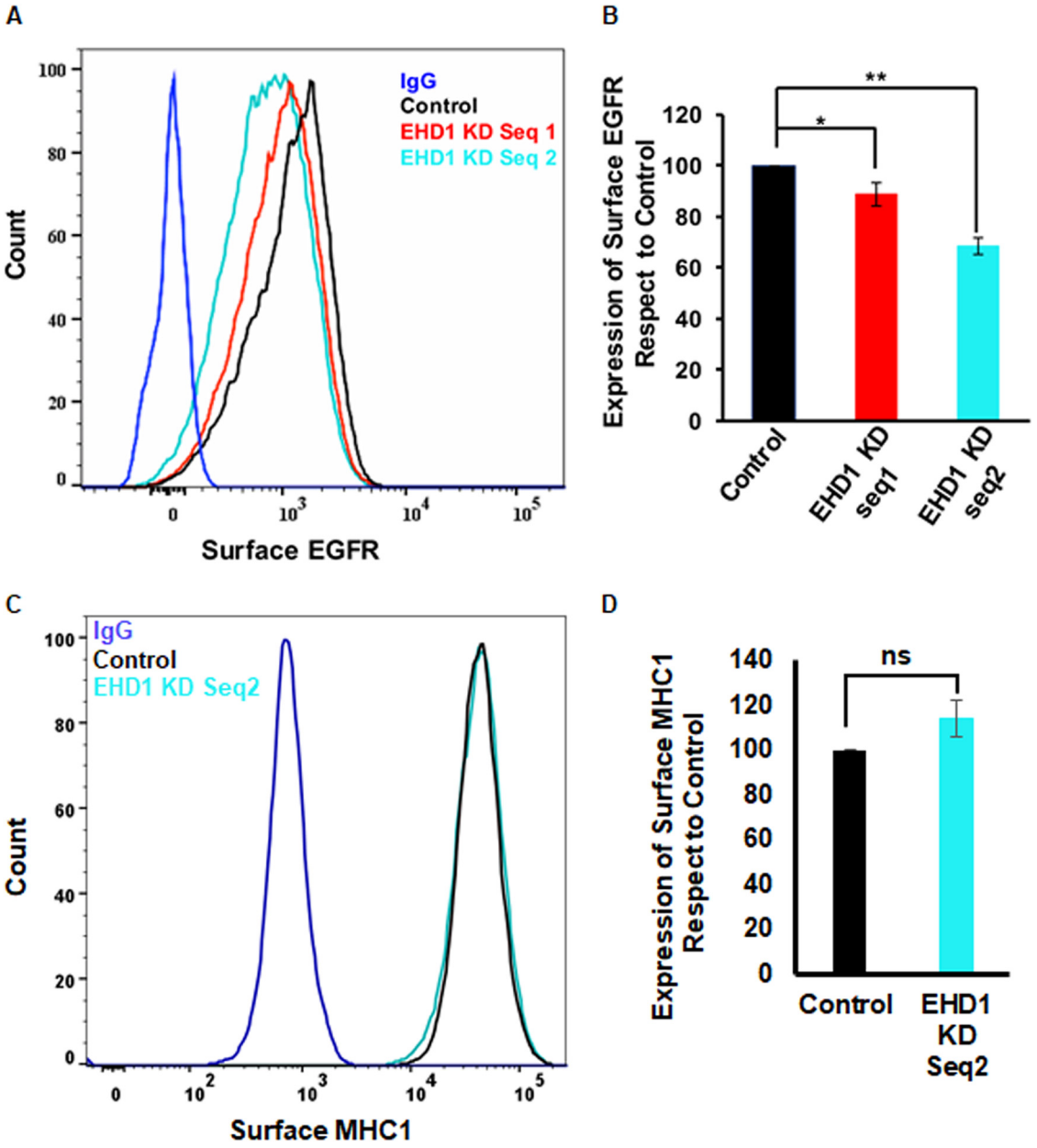


**FIG 2** EHD1 knockdown leads to reduction in the cell surface EGFR levels in 16A5 cells. (A) Reduction in cell surface EGFR upon EHD1 KD in 16A5 cells analyzed by FACS. 16A5 cells stably transduced with Dox-inducible nontargeting or EHD1-targeted shRNA (Seq. 1 or Seq. 2) were cultured under steady-state for 2 days prior to a 24-h EGF and serum deprivation with Dox present all the time. Live cells were analyzed by FACS for surface expression of EGFR. (B) Quantification of mean fluorescence intensities of results presented in panel A. Values are means plus standard errors of the means for $n = 4$. *, $P < 0.05$; **, $P < 0.02$; ns, not significant. (C) EHD1 KD did not reduce surface MHC class I (MHC-I) levels on 16A5 cells. 16A5 cells stably transduced with Dox-inducible nontargeting or EHD1-targeted shRNAs (Seq. 2) were cultured as described for panel A and analyzed by FACS for cell surface levels of MHC-I. (D) Quantification of mean fluorescence intensities of results presented in panel C. Values are means plus standard errors of the means for $n = 3$.

**EHD1 and EGFR colocalize in intracellular vesicular structure.** Given the impact of EHD1 depletion on the total and cell surface levels of unstimulated EGFR, we considered the possibility that EHD1 regulates the intracellular trafficking of EGFR. To determine whether EHD1 colocalizes with EGFR, 16A5 cells were deprived of serum and EGF for 6 h in the presence of either dimethyl sulfoxide (DMSO) or 10 $\mu$M monensin and subjected to immunofluorescence costaining of endogenous EGFR and EHD1. Monensin treatment was included as we previously found it to enhance the colocalization of lung cancer-associated EGFR mutants with EHD1 in the endocytic recycling compart-

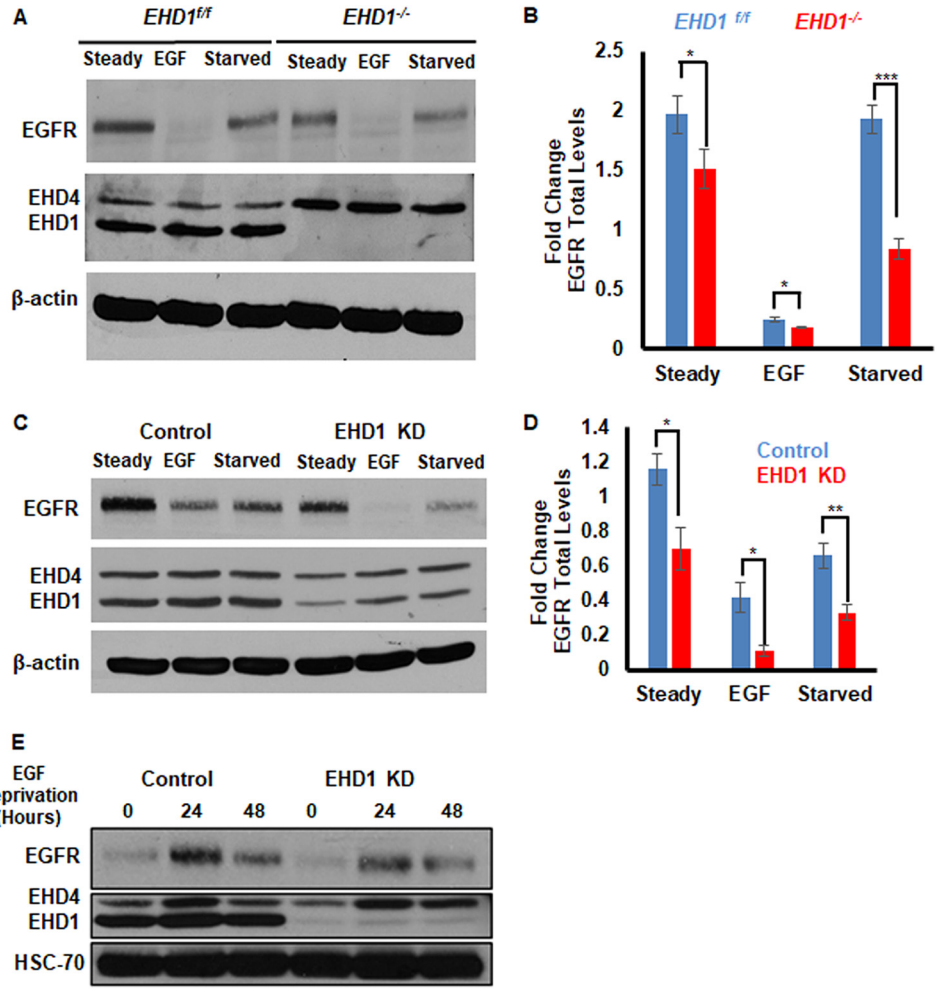


**FIG 3** EHD1 knockout or knockdown in additional cell types leads to reduced EGFR levels under ligand-free culture. (A) Reduction in EGFR level in EHD1 knockout MEFs. EHD1$^{flox/flox}$ (EHD1$^{f/f}$) and EHD1$^{-/-}$ MEFs were cultured in the presence of 2 nM EGF for 4.5 h to promote EGFR degradation and switched to serum starvation medium to assess the accumulation of EGFR. Lysates were blotted for EGFR, EHD1/4 and $\beta$-actin. (B) Densitometric quantification of EGFR signals presented in panel A normalized to the value of the $\beta$-actin loading control ($n = 3$). *, $P < 0.05$; ***, $P < 0.001$. (C) Reduction in EGFR level by EHD1 KD in MDA-MB-231 breast cancer cell line. MDA-MB-231 triple-negative breast cancer cells stably expressing nontargeting control or EHD1-targeted (Seq. 1) Dox-inducible shRNAs were pretreated with Dox for 2 days, stimulated with 2 nM EGF for 4.5 h to deplete the EGFR protein, and switched to low-serum medium without EGF to assess the EGFR accumulation by Western blotting of lysates. (D) Densitometric quantification of EGFR signals presented in panel C normalized to the level of the $\beta$-actin loading control ($n = 3$). *, $P < 0.05$; **, $P < 0.02$. (E) Reduction in EGFR levels by EHD1 KD in the S2013 pancreatic cancer cell line. S2013 pancreatic adenocarcinoma cells were transiently transfected with a nontargeting (control) or EHD1-targeted siRNA, and cells were treated as described for MDA-MB-231 cells in panel C, followed by Western blotting of lysates for EGFR, EHD1/4, and HSC-70.

ment (42). Consistent with previous reports using other cell types (63), monensin treatment of 16A5 cells increased the accumulation of EGFR in perinuclear vesicles, indicating an effective inhibition of cargo exit from endocytic compartments. EHD1$^+$/EGFR$^+$ vesicles were observed as sparse puncta in DMSO-treated cells (Fig. 4A); however, a clear perinuclear EHD1 and EGFR colocalization was observed in monensin-treated cells (Fig. 4B). When an exogenous EHD1-DsRed construct was expressed via transient transfection, the colocalization with endogenous EGFR became obvious even in the absence of monensin treatment (Fig. 4C) and was more robust in monensin-treated cells (Fig. 4D). Since cells in regular culture (in EGF-containing medium) showed little surface and intracellular staining and barely detectable EGFR by blotting (Fig. 1C), the accumulation of cell surface EGFR upon removal of EGF is likely to be largely dependent on transport from the Golgi compartment to the cell surface of newly

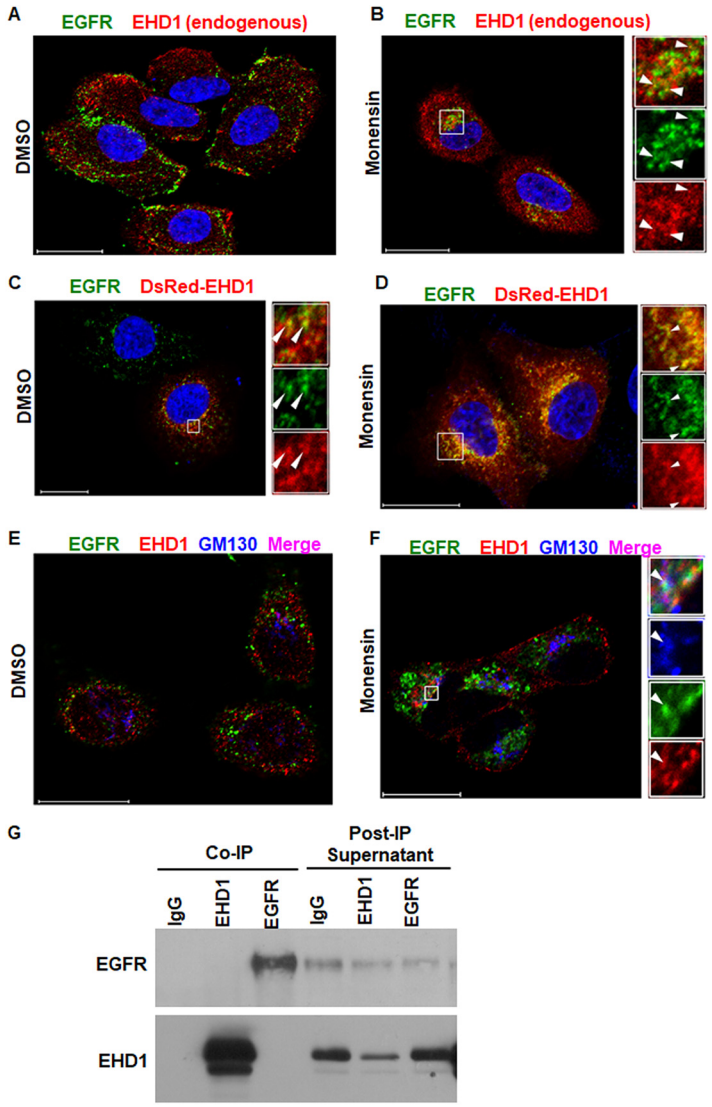


**FIG 4** EHD1 and EGFR colocalization in intracellular vesicular structures. Nontransfected or transiently DsRed-EHD1-transfected 16A5 cells were subjected to serum and EGFR deprivation for 6 h and concurrently treated with DMSO or monensin (10 $\mu$M), followed by immunofluorescence staining of fixed and permeabilized cells for EGFR (green) or GM130 (blue). Colocalization is indicated by arrowheads in the insets on the right. (A and B) Localization of endogenous EHD1 and EGFR in DMSO- and monensin-treated nontransfected 16A5 cells. Nuclei were stained with 4′,6′-diamidino-2-phenylindole (blue). (C and D) Localization of transfected DsRed-EHD1 and endogenous EGFR in DMSO-treated and monensin-treated 16A5 cells. Nuclei are stained with 4′,6′-diamidino-2-phenylindole (blue). (E and F) Localization of transfected DsRed-EHD1 and endogenous EGFR and GM130 (blue) in 16A5 cells treated with 4′,6′-diamidino-2-phenylindole and monensin treated. Serial z-sections were obtained to validate the colocalization, which is shown in an orthogonal view. Scale bars, 5 $\mu$m. (G) Lack of coimmunoprecipitation between EHD1 and EGFR. 16A5 cells were serum and EGF deprived for 24 h, and 1-mg aliquots of protein lysate were subjected to immunoprecipitation with control antibody, anti-EGFR antibody, or anti-EHD1 antibody. Prior to washing the protein G- or A-Sepharose beads used for capture of IPs, aliquots of the supernatant equivalent to 5% of the lysate used for IPs were saved and concurrently run alongside the IPs, and immunoblotting for EGFR or EHD1 was performed. Note a lack of co-IP between EHD1 and EGFR; supernatants indicate effective depletion of the cognate proteins during IP, as expected. The remnant of the band in the IP next to the last lane is due to cropping out a positive-control band for EHD1.

synthesized EGFR. Thus, we reasoned that EHD1 may function in part by regulating EGFR trafficking at the Golgi apparatus. Three-color confocal immunofluorescence staining of endogenous EGFR and the Golgi marker GM130 with ectopically expressed EHD1-DsRed demonstrated that a pool of EHD1 and EGFR was colocalized at the Golgi compartment (Fig. 4E and F). In view of the colocalization of EHD1 and EGFR, we asked

if the two proteins physically associate with each other. To this end, we carried out anti-EHD1 or anti-EGFR immunoprecipitations (IPs) from lysates of EGF-deprived 16A5 cells, followed by immunoblotting for EGFR or EHD1, respectively. In each case, efficient IP of EHD1 or EGFR was established by immunoblotting for the cognate protein and by its depletion in the supernatants remaining after IP (Fig. 4G). No co-IP between EHD1 and EGFR, however, was observed. Thus, while EHD1 and EGFR do not appear to physically interact, they colocalize in intracellular compartments, consistent with a role of EHD1 in the intracellular traffic of EGFR.

**EHD1 knockdown results in EGFR retention in the Golgi apparatus.** Given the EGFR and EHD1 colocalization at the Golgi apparatus, we asked if EHD1 functions in EGFR trafficking out of the Golgi compartment, using the inducible knockdown and EHD1-GFP rescue 16A5 cell lines. Cells were switched from regular, EGF-containing medium to a serum- and EGF-free medium and analyzed for EGFR localization at various time points up to 24 h using confocal imaging. Under steady-state conditions, weak EGFR (green) signals seen at time zero were predominantly intracellular, partly localizing to the perinuclear area (Fig. 5A). In EHD1-GFP-expressing rescue cells, some perinuclear EGFR colocalized with EHD1 (pseudocolored red). Upon EGF removal from the medium, EGFR in the control cell line (no Dox treatment) and in the EHD1-GFP rescue cell line (treated with Dox) progressively localized to the cell surface, as expected. In contrast, cells with EHD1 KD but without EHD1 rescue exhibited strong perinuclear EGFR accumulation with correspondingly lower surface EGFR signals (Fig. 5A). This perinuclear compartment was identified as the Golgi compartment, based on GM130$^+$ costaining (Fig. 5B).

IPs with an antibody that recognizes the mature EGFR (clone 528) (64) from lysates of cells that were metabolically pulse-labeled with [$^{35}$S]methionine-cysteine and chased in label-free medium for the indicated times (0, 30, 90, or 270 min) revealed that a smaller fraction of the newly synthesized EGFR was converted to the mature form in EHD1 KD 16A5 cells and with a delay (Fig. 5C). The increase in radiolabel during the 4-h chase in control cells (Fig. 5C) is consistent with the EGFR becoming more antibody reactive as the receptor undergoes posttranslational modification, as shown previously (65, 66).

The Golgi retention of EGFR in EHD1-depleted cells following a switch to EGF-free medium and the results of metabolic pulse-chase analyses support a role of EHD1 in anterograde trafficking of EGFR out of the Golgi compartment. However, given the recently identified roles of EHD proteins in retrograde trafficking of endocytic cargo, we assessed if EGFR undergoes retrograde trafficking from the cell surface in the absence of ligand stimulation and whether this process is defective in EHD1 KD cells. Previous studies of nuclear localization of EGFR have concluded that EGFR traffics via a retrograde endocytic route, but such studies were done in the presence of ligands (67). Cells cultured with or without Dox were subjected to serum and EGF deprivation for 6 h and chilled on ice for 20 min, and live cells on ice were stained with a biotinylated anti-EGFR antibody to visualize the internalized EGFR with fluorescein isothiocyanate (FITC)-conjugated NeutrAvidin (Fig. 5D, pulsed). Cells were then rinsed with ice-cold phosphate-buffered saline (PBS) and incubated at 37°C for 18 h in serum- and EGF-free medium before fixation. Cells without prestaining of the surface EGFR were processed in parallel (Fig. 5D, not pulsed). Fixed cells were permeabilized and stained for GM130 and the recycling endosome marker Rab11 (68). Control cells that were not prestained with anti-EGFR–biotin were also stained for EGFR. Under these conditions, we observed that EGFR prelabeled at the cell surface accumulated in a GM130/Rab11 double-positive, perinuclear compartment in EHD1 KD cells, as also seen in cells that were not prelabeled on the cell surface (Fig. 5D). Very little surface-labeled EGFR was seen to accumulate in the same compartment in control cells (Fig. 5D). This result indicates that EHD1 also regulates the exit of the EGFR pool that enters the Golgi compartment after endocytosis and retrograde transport from the cell surface.

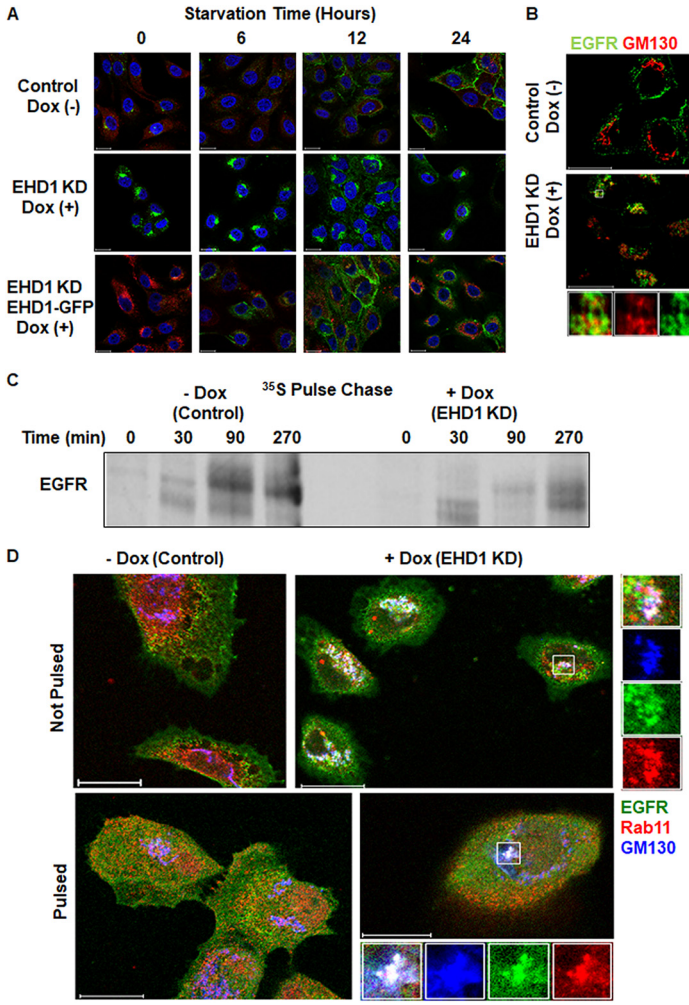


**FIG 5** EHD1 knockdown leads to EGFR retention in the Golgi apparatus. (A) Perinuclear accumulation of EGFR upon EHD1 KD in 16A5 cells and rescue of the defect by exogenous EHD1. 16A5 cells expressing Dox-inducible EHD1 shRNA (Seq. 1) were cultured without [Control Dox (−)] or with [EHD1 KD Dox (+)] Dox, or the same cells stably expressing Dox-inducible EHD1-GFP were cultured with Dox, as indicated. Cells were then switched to Dox with or without serum and EGF deprivation medium (starvation) for the indicated times, followed by staining for EGFR (green in the top and middle panels; red, pseudocolored green, in the bottom panel), EHD1 (red; top and middle panels), GFP (bottom panel; pseudocolored red), and nuclei (4′,6′-diamidino-2-phenylindole; blue) and subjected to confocal imaging. Note the accumulation of EGFR (green) in an intracellular compartment upon starvation under the EHD1 KD condition (middle panel; reduced red staining) and rescue of this phenotype by EHD-1 GFP (pseudocolored red; bottom panel). (B) Perinuclear EGFR in EHD1 KD 16A5 cells colocalizes with Golgi marker GM130. Intracellular EGFR colocalizes with GM130 upon EHD1 KD [Dox (+)] in contrast to results for the control [Dox (−)]. Dox treatment and serum and EGF deprivation for 24 h were performed as described for panel A. (C) Delayed maturation of newly synthesized EGFR upon EHD1 knockdown. 16A5 cells stably expressing a Dox-inducible EHD1 shRNA and cultured without (−Dox) or with (+Dox) Dox were metabolically pulse-labeled with [$^{35}$S]methionine-cysteine, followed by chase for the indicated times. Anti-EGFR immunoprecipitates using antibody 528 were imaged by fluorography. A representative of three experiments is shown. (D) EHD1 KD in 16A5 cells impairs the retrograde trafficking of surface EGFR to the Golgi compartment Cells cultured with or without Dox were subjected to serum and EGF deprivation for 6 h and chilled on ice for 20 min, and live cells were stained with a biotinylated anti-EGFR antibody on ice (pulsed). Cells were rinsed with ice-cold PBS and incubated at 37°C for 18 h in serum- and EGF-free medium before fixation. Cells without surface EGFR staining were processed in parallel (not pulsed). Cells were fixed, permeabilized, and stained as before for GM130 and Rab11 and for EGFR in cells that were not previously stained with anti-EGFR–biotin. Biotinylated antibody against EGFR was visualized with FITC-conjugated NeutrAvidin.

**EHD1 knockdown reduces the EGF-dependent cell proliferation.** To assess the functional consequences of EHD1 KD in MECs, we first examined if the reduction in EGFR levels upon EHD1 KD was accompanied by reduced downstream signaling output. Indeed, EHD1 KD 16A5 cells exhibited substantially reduced EGFR phosphory-

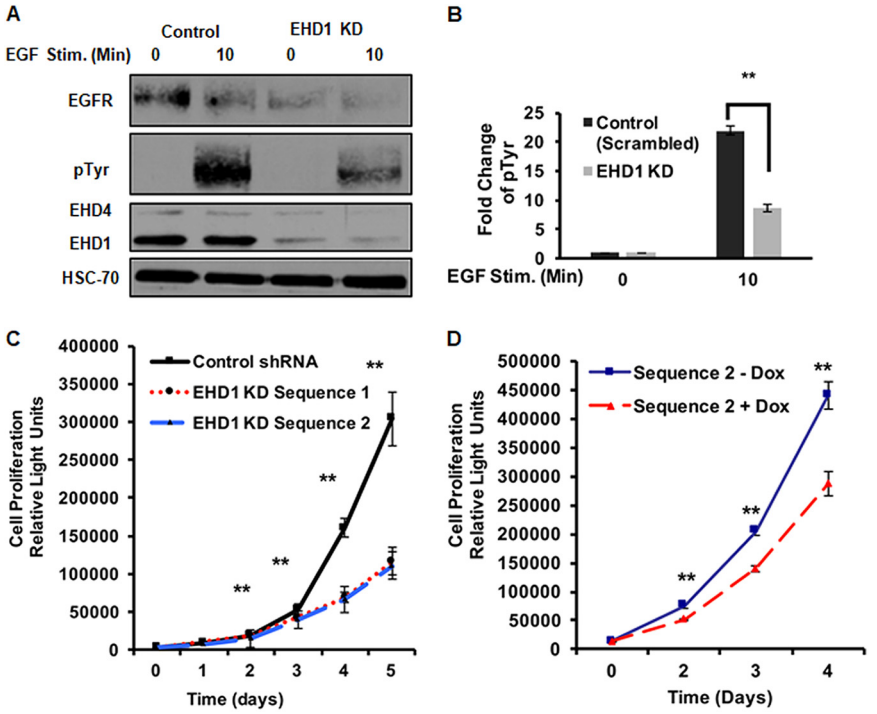


**FIG 6** EHD1 knockdown reduces EGF-dependent cell signaling and cell proliferation. (A) EHD1 KD impairs the EGF-induced tyrosine phosphorylation of EGFR. 16A5 cells were transiently transfected with a control or EHD1 3′ UTR-targeted siRNA, and cells were EGF and serum starved for 48 h, followed by EGF (2 nM) stimulation (Stim) for 10 min; lysates were then blotted for EGFR, phosphotyrosine (pTyr), EHD1/4, and HSC-70. The major band in the phosphotyrosine blot corresponds to phosphorylated EGFR. (B) Densitometric quantification of phosphorylated EGFR bands presented in panel A, normalized to the level of HSC-70 ($n = 3$). **, $P < 0.02$. (C and D) Impaired EGF-induced proliferation of 16A5 cells upon EHD1 KD. A total of 1,500 16A5 cells expressing a nontargeting control shRNA or EHD1 shRNA (Seq. 1 or 2) were plated in the inner wells of 96-well plates (60 replicates/time point) and cultured in EGF (2 nM)-containing medium for 5 days in the presence of Dox. Cell proliferation was assessed on each day using a CellTiter-Glo assay (C). 16A5 cells expressing EHD1 shRNA (Seq. 2) were cultured in EGF-containing medium without (−) or with (+) Dox, and a CellTiter-Glo assay was performed on the indicated days (60 replicates per time point) (D). **, $P < 0.02$, by Student's *t* test.

lation upon stimulation with EGF, as visualized by phosphotyrosine immunoblotting of cell lysates (Fig. 6A and B). In view of reduced ligand-induced EGFR phosphorylation seen upon EHD1 depletion, we compared the time course of EGF-induced proliferation of 16A5 cells with or without EHD1 KD, using a CellTiter-Glo assay. Cells engineered with two distinct Dox-inducible EHD1 shRNAs or a control shRNA were kept in Dox for the duration of the experiment. Both EHD1 KD 16A5 lines displayed significantly reduced proliferation relative to that of control shRNA-expressing cells (Fig. 6C). These results were confirmed by assessing the proliferation of Dox-inducible EHD1 KD 16A5 cells upon culture with and without Dox (Fig. 6D).

**RUSC2 is a novel potential EHD1 partner that colocalizes with EGFR at the Golgi compartment.** In view of our findings that EHD1 plays a key positive role in the cell surface expression of unstimulated EGFR, we were intrigued by a proteomics analysis of unstimulated EGFR-associated protein complex in which RUSC2 was reported as an uncharacterized component (53). We noted two potential EHD1 EH domain-binding NPF motifs in RUSC2 (amino acids 43-NPFCPPELG-51 and 101-NPFLL QEGV-109) which bound with moderate affinity to the EH domain of EHD1 in an *in vitro* fluorescence polarization-based competition assay using a labeled peptide derived from MICAL-like 1 protein (amino acids 425-NPFEEEEED-433) as a probe (Fig. 7A). Using an antibody generated against a human RUSC2 peptide (see Materials and Methods), we found that RUSC2 was expressed in 16A5 cells. However, we could not detect the binding of full-length RUSC2 with the EHD1 EH domain, nor could we detect co-IP of

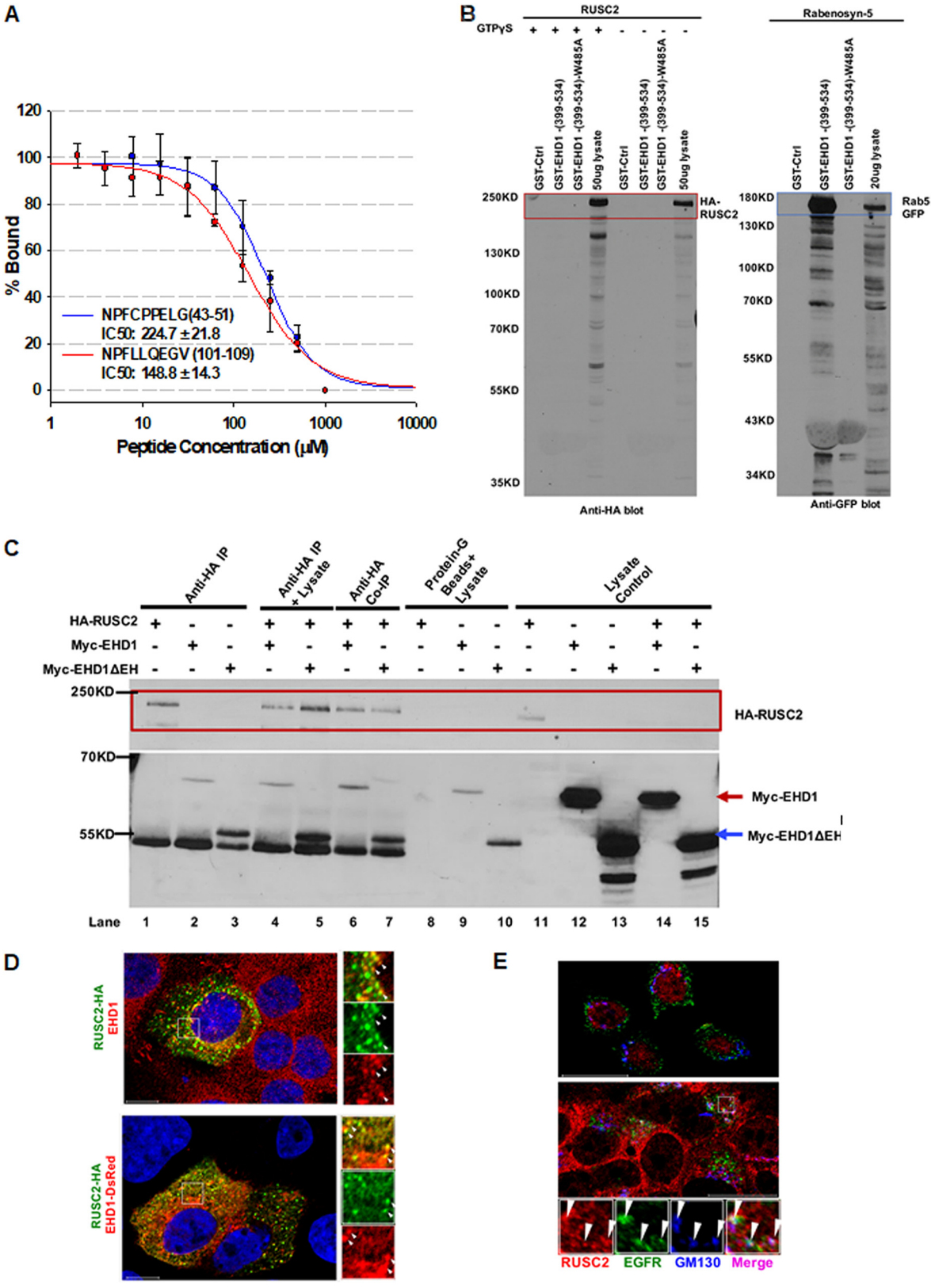


**FIG 7** Identification of RUSC2 as a potential EHD1 partner and its colocalization with EGFR at the Golgi compartment. (A) EHD1 EH domain binding to RUSC2 NPF-containing motifs *in vitro*. The binding of two nonameric peptides corresponding to NPF-containing sequences in RUSC2 (amino acids 43-NPFCPPELG-51 and 101-NPFLLQEGV-109) to purified recombinant GST-EHD1 EH domain was assessed in an *in vitro* fluorescence polarization competition assay using competition binding of a labeled peptide derived from MICAL-like 1 protein (amino acids

(Continued on next page)

ectopically cotransfected EHD1 and RUSC2, either when immunoprecipitated hemagglutinin (HA)-RUSC2 was incubated with lysates of cells transfected with Myc-EHD1 or when HA-RUSC2 and Myc-EHD1 were cotransfected in HEK-293T cells (Fig. 7B and C).

To determine if RUSC2 and EHD1 colocalize in intracellular vesicles, we first assessed the colocalization of endogenous EHD1 and RUSC2; the anti-RUSC2 antibody, however, proved suboptimal for imaging of endogenous RUSC2. We therefore cotransfected the EHD1-DsRed and HA-RUSC2 constructs into 16A5 cells to assess their colocalization by confocal imaging. Colocalization was observed when either endogenous EHD1 was immunostained along with exogenous HA-RUSC2 (Fig. 7D, top panel) or when HA-RUSC2 and EHD1-DsRed were examined (Fig. 7D, bottom panel). Vesicular and tubular HA-RUSC2 displayed a tight correlation with DsRed-EHD1 localized to similar structures (Fig. 7D, bottom panel).

Given the previous reports that RUSC2 directly interacts with GM130 as well as with Golgi-associated Rab1 (50), the prominent colocalization of RUSC2 with EHD1 led us to hypothesize that RUSC2, similar to EHD1, may function to promote the EGFR trafficking out of the Golgi compartment. We first assessed whether RUSC2 localizes in the Golgi compartment where EGFR accumulates upon EHD1 KD. Indeed, we observed significant three-color colocalization between EGFR, RUSC2, and GM130 upon EHD1 KD (Fig. 7E).

**RUSC2 knockdown phenocopies the effects of EHD1 depletion on basal, unstimulated EGFR expression.** Given the above results, the reported RUSC2 interaction with GM130 (50) and the role of RUSC2-interacting small G-protein Rab1a in regulating trafficking from the Golgi compartment to the plasma membrane (50, 69, 70), we reasoned that RUSC2 may also function in EHD1-dependent EGFR trafficking out of the Golgi compartment. To test this idea, 16A5 cell lines expressing Dox-inducible shRNAs targeting RUSC2 were cultured in regular EGF-containing medium in the presence of Dox for 3 days to achieve RUSC2 KD. The cells were then cultured in serum- and EGF-free medium, and the accumulation of total EGFR levels over a 24-h time course was monitored using Western blotting. RUSC2 KD, using two independent shRNAs, led to a substantial impairment of the accumulation of total EGFR protein upon EGF withdrawal compared to levels in control cells; this effect was even more robust than that seen with EHD1 KD (Fig. 8A and B). Flow cytometry analyses of cells treated with Dox for 48 h in EGF-containing medium followed by Dox in serum and EGF deprivation medium for 24 h revealed a significant decrease in the cell surface EGFR levels in RUSC2 KD cells compared to levels in control cells, mimicking the impact of EHD1 KD (Fig. 8C and D).

**FIG 7** Legend (Continued)
425-NPFEEEEED-433). $IC_{50}$, 50% inhibitory concentration. (B) Lack of EHD1 EH domain pulldown of full-length RUSC2 in cell lysates. Five-milligram protein aliquots of lysates of HEK-293T cells transiently transfected with HA-RUSC2, supplemented or not supplemented with GTP$\gamma$S (300 $\mu$M), were used for pulldown with 50 $\mu$g of purified GST fusion proteins: GST-Ctrl, GST–EHD1-(399–534), and GST–EHD1-(399–534)-W485A (nonbinding point mutant), immobilized on glutathione-Sepharose beads. Binding reactions or lysate control were subjected to anti-HA immunoblotting to detect RUSC2 (left panel). No RUSC2 pulldown with a GST EH domain was seen. Similar analysis of rabenosyn-5-transfected cell lysates (right panel) showed the expected pulldown with the wild-type but not the mutant GST-EHD1 EH fusion protein. (C) Lack of binding between full-length RUSC2 and EHD1. HEK-293T cells were either separately transfected with HA-RUSC2, Myc-tagged full-length EHD1 (Myc-EHD1), or EH domain-deleted EHD1 (Myc–EHD1-ΔEH) (lanes 1 to 5, 8 to 10, and 11 to 13) or cotransfected with HA-RUSC2 and Myc-EHD1 or Myc–EHD1-ΔEH (lanes 6, 7, 14, and 15). Lysates of cells singly transfected with the indicated proteins were subjected to anti-HA IP from 1-mg aliquots of protein lysate (lanes 1 to 3), or protein G-Sepharose beads containing HA-RUSC2 immunoprecipitated from 1-mg aliquots of protein lysate of HA-RUSC2 singly transfected cells were further incubated with 1-mg lysates of cells transfected with Myc-EHD1 (lane 4) or Myc–EHD1-ΔEH (lane 5). The binding reactions were immunoblotted with anti-HA (upper) or anti-Myc (lower) antibodies. Anti-HA IPs from lysates of cotransfected cells (lanes 6 and 7) were also subjected to anti-HA and anti-Myc blotting along with whole-cell lysates (lanes 11 to 15). As additional controls, lysates of singly transfected cells without anti-HA IP were incubated with protein G-Sepharose beads and immunoblotted as described for the binding reactions (lanes 8 to 10). HA-RUSC2 is shown in a red box; Myc-EHD1 and Myc–EHD1-ΔEH are indicated by red and blue arrows, respectively. No binding between EHD1 and RUSC2 was seen using the two-step binding approach or co-IP from doubly transfected cells. The Myc-EHD1 and Myc–EHD1-ΔEH bands seen in the binding reaction reflect nonspecific binding to protein G beads, as shown by the presence of these bands in incubations of protein G beads plus lysate. (D) Colocalization of EHD1 and RUSC2 in 16A5 cells. 16A5 cells transiently transfected with HA-RUSC2 were either used as such for costaining with anti-HA (green) and anti-EHD1 (endogenous EHD1; red) antibodies or were transiently cotransfected with EHD1-DsRed (bottom panel) and stained with anti-HA (green). Nuclei are visualized with 4′,6′-diamidino-2-phenylindole (blue). (E) RUSC2 colocalizes with EGFR. 16A5 cells with a Dox-inducible EHD1 shRNA (Seq. 1) were transiently transfected with HA-RUSC2 and cultured in the presence of Dox for 48 h to induce the EHD1 KD (and thus Golgi retention of EGFR), switched to serum- and EGF-deprived medium for 24 h, and stained with anti-RUSC2 (red), anti-EGFR (green), and anti-GM130 (blue) antibodies. Insets at higher magnification are shown to highlight the colocalization.

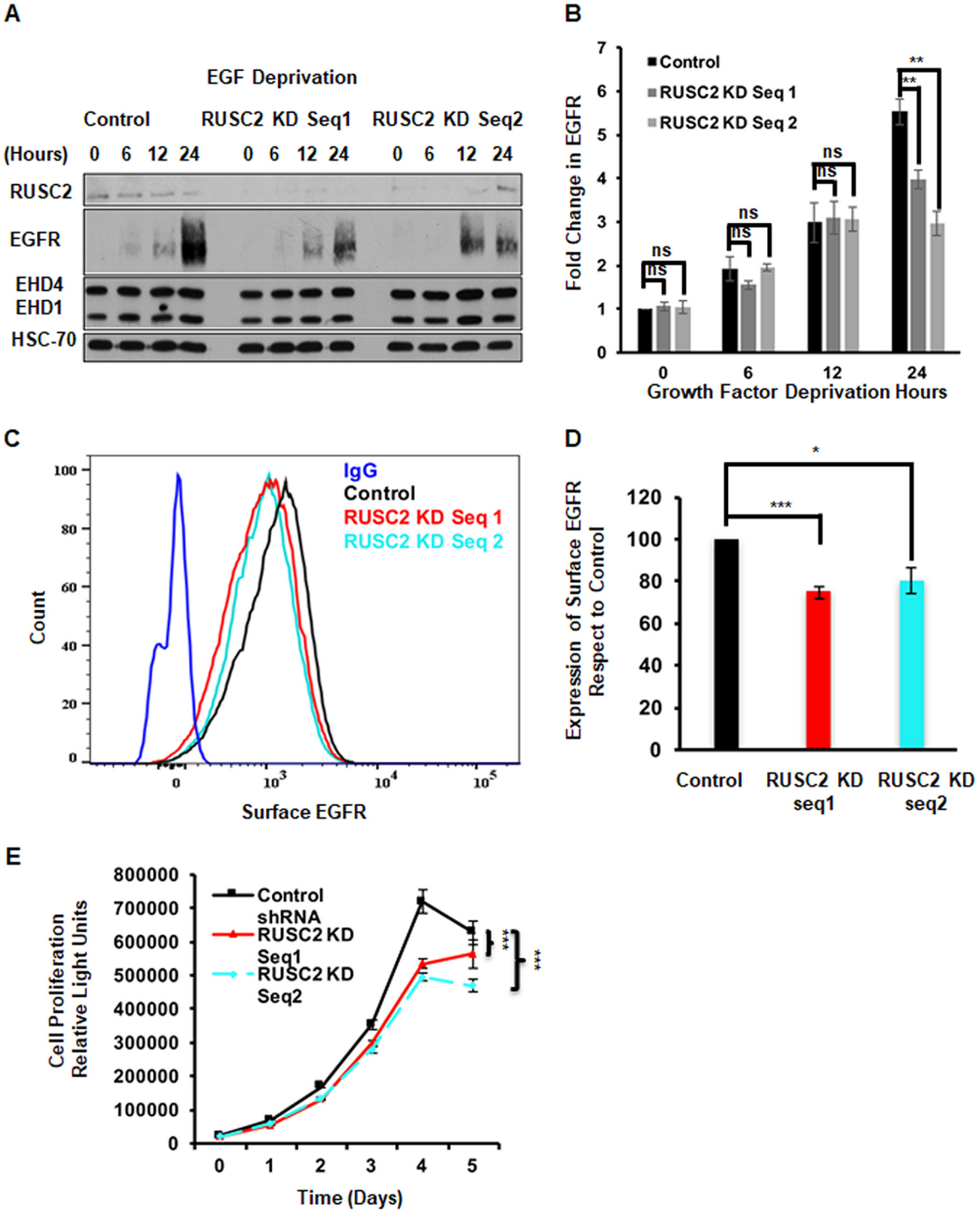


**FIG 8** RUSC2 knockdown phenocopies the effects of EHD1 depletion on basal, unstimulated EGFR expression. (A) RUSC2 KD impairs the accumulation of EGFR when cells are switched to EGF-deprived medium. 16A5 cells stably expressing a Dox-inducible nontargeting (control) or RUSC2-targeted (Seq. 1 or 2) shRNA were cultured in the presence of Dox for 3 days before being switched to serum and EGF deprivation medium for the indicated times, followed by analysis of lysates by immunoblotting for EGFR, RUSC2, EHD1/4, and HSC-70 (loading control). RUSC2 KD has no impact on EHD1/4 levels. (B) Densitometric quantification of EGFR signals shown in panel A, normalized to the level of HSC-70 ($n = 3$). **, $P < 0.02$. (C) RUSC2 KD reduced the cell surface EGFR levels. Live-cell FACS analysis of surface EGFR levels on 16A5 cells expressing a Dox-inducible nontargeting (Control) or RUSC2-targeted (Seq. 1 or 2) shRNA after 3 days of DOX pretreatment, with the last 24-h culture in serum- and EGF-deprived medium with Dox. (D) Quantification of EGFR staining data shown in panel C. Values on the *y* axis represent MFI data normalized to the level of Ig staining. Control shRNA EGFR levels are set as 100%. Error bars indicate standard errors of the means, and statistical significance was calculated using Student's *t* test ($n = 3$). Each experimental condition represents FACS analysis of 100,000 cells. *, $P < 0.05$; ***, $P < 0.001$. (E) RUSC2 KD impairs EGF-driven cell proliferation. 16A5 cell lines expressing the Dox-inducible control or RUSC2-targeted (Seq. 1 or 2) shRNA were plated at 1,500 cells per well (60 replicates per time point) and cultured for 5 days in the presence of Dox. Cell proliferation was assessed on each day using a CellTiter-Glo assay ***, $P < 0.001$, by Student's *t* test.

To determine the functional consequences of the reduced cell surface EGFR expression upon RUSC2 KD, we cultured 16A5 cell lines expressing two distinct Dox-inducible RUSC2 shRNAs in the presence of Dox for 5 days and assessed the impact of RUSC2 depletion on cell proliferation. Indeed, RUSC2 KD led to a significant reduction in EGF-induced cell proliferation relative to the level in control shRNA cells (Fig. 8E).

Collectively, these results support our conclusion that RUSC2 and EHD1 function in a common pathway to positively regulate the basal traffic of EGFR from the Golgi compartment to the cell surface to ensure optimal surface receptor levels for subsequent ligand-mediated activation and cellular responses.

## DISCUSSION

Growth factor receptor tyrosine kinase activation provides a fundamental mechanism to regulate cellular activities under varied physiological conditions. Expression of a cell-type-dependent level of a given RTK is a prerequisite for the appropriate levels of cellular responses to cognate ligands, and many RTKs are now known to attain oncogenic properties through overexpression, mutations, or aberrant ligand availability. Surface expression of RTKs is indeed a requisite for oncogenesis (71). Yet relatively little is known about the mechanisms that ensure proper display of activation-ready RTKs on the cell surface to ensure physiological or oncogenic signaling upon ligand-induced activation. Here, we use EGFR, expressed on the nontumorigenic EGF-dependent immortal human mammary epithelial cell line 16A5, to identify a novel role of the endocytic recycling regulator EHD1 and of a little-understood Rab effector protein, RUSC2, in the maintenance of the cell surface display of EGFR by controlling its trafficking at the Golgi compartment. While EHD1 and its family members have emerged as key regulators of intracellular trafficking of internalized cell surface receptors (72), including in some cases the retrograde trafficking to the Golgi compartment (73, 74), our studies provide evidence for a novel and functionally important role of EHD1 in the anterograde trafficking of EGFR from the Golgi compartment to the cell surface.

By immunofluorescence analyses, we found that cells deprived of EGFR ligands exhibit EGFR localization to EHD1$^+$ vesicular structures that are also positive for the Golgi marker GM130 (Fig. 5B). We demonstrate that EHD1 depletion leads to accumulation of EGFR in this compartment, with concurrent reduction in the trafficking of EGFR to the cell surface (Fig. 5A). Since EHD1 is currently thought to work primarily at the endosomes, we tested and found support for the idea that a portion of the Golgi compartment-localized EGFR is derived from the pool internalized from the cell surface (Fig. 5A). However, our results indicate that much of the Golgi compartment-localized EGFR represents the newly synthesized protein on its way to the cell surface (Fig. 5C). As our analyses show, the total and cell surface levels of EGFR under steady-state culture in EGF-containing medium are low, as expected from the EGF-induced and Cbl family ubiquitin ligase-dependent lysosomal degradation of activated EGFR (60). We therefore deliberately carried out analyses in which such steady-state cultures were switched to EGF-free medium to allow the newly synthesized EGFR to traffic to, and accumulate at, the cell surface. A block in the transit of EGFR out of the Golgi compartment under EHD1 KD conditions was clear under these conditions (Fig. 5A). Furthermore, the appearance of a fully mature form of the newly synthesized EGFR was delayed in EHD1 KD cells (Fig. 5C). The impact of EHD1 depletion was also observed in multiple other cell types, including MEFs in which the endogenous floxed EHD1 was conditionally deleted (Fig. 3), albeit the impact was modest in these other cell systems. The differences in the extents to which EGFR levels are impacted by EHD1 depletion may relate to the requirement of EGFR signaling for growth of the immortal MEC line 16A5 used in most of our experiments (55), while the other cell systems are not dependent on EGFR signals for *in vitro* growth. This idea is consistent with a robust reduction in CSF1R expression in EHD1-null murine macrophages (41). Alternatively, other EHD family members may play a more significant redundant role in these other cell types. Notably, EHD4 levels are substantially increased in MEFs with EHD1 deple-

tion, and future analyses using MEFs with double EHD1/EHD4 depletion should be instructive in this regard. Overall, our results support a key role of EHD1 in promoting the exit of unstimulated EGFR out of the Golgi compartment as a mechanism to ensure that optimal EGFR levels are maintained at the cell surface for the physiological activation of cells through this receptor. Indeed, we demonstrate that the reduced levels and surface display of EGFR in EHD1 KD cells translate into impaired signaling and cell proliferation (Fig. 6).

Importantly, since we show that cell surface EGFR (labeled on the cell surface with an antibody) also gains entry into an EHD1$^+$/GM130$^+$ compartment, apparently reflecting its retrograde trafficking to Golgi compartment, and that EHD1 KD caused a more significant Golgi retention of this cohort as well (Fig. 5A), it is likely that unstimulated EGFR transported through both anterograde and retrograde mechanisms reaches an EHD1-dependent Golgi compartment and that EHD1 is required for EGFR to be recycled to the cell surface from this compartment. Intermixing of biosynthetic and endocytic cargos of cell surface receptors has been thought to primarily occur in the sorting endosomes, which then direct these receptors to various subcellular destinations (75). Thus, the control of endocytic as well as biosynthetic pools of a prototype RTK at the Golgi compartment is unprecedented. It is notable that EHD1 knockdown was shown to impair the biosynthetic transport of a vesicular stomatitis virus G protein (VSVG)-GFP fusion protein used as a marker of the transport from the Golgi compartment to the cell surface (73), but no further studies along these lines have been reported.

Clearly, the EHD1-dependent control of EGFR trafficking described here is functionally important, as we demonstrate, and it will be of great interest to determine if this mechanism applies broadly to other RTKs and possibly other cell surface receptors. Consistent with a broader role of EHD1 in RTK trafficking, we have recently found that EHD1 also plays a key role in the surface expression of the CSF1R, an RTK, on primary macrophages (41). Notably, however, we did not observe a significant impact of EHD1 depletion on MHC-I cell surface expression when this was examined under the same conditions as we used for analyses of EGFR (ligand-free culture), suggesting that our findings may be more relevant to RTKs whose cell surface pools are subject to rapid ligand-induced degradation and require efficient surface delivery through new synthesis. Our inability to show an impact of EHD1 depletion on surface MHC-I levels is likely to reflect our methodology (designed to detect the trafficking of newly synthesized RTKs) since endocytic recycling of MHC-I, tracked using antibody binding at the cell surface, is known to be impaired upon EHD1 KD (23). While our studies have focused on EHD1, it will be important in future studies to assess any roles of the other EHD family members in the Golgi compartment-to-surface exit of EGFR and other RTKs, given their redundant roles that we have observed in other biological systems (34, 76, 77).

In addition to demonstrating a novel functional role of EHD1 in EGFR trafficking out of the Golgi compartment, our studies reveal a new potential EHD1 partner, RUSC2, that is involved in this process (Fig. 7 and 8). RUSC2 is a little-studied member of a small family of RUN domain-containing proteins that include RUSC1/NESCA (new molecule containing SH3 at the carboxy terminus) with which it displays ~30% overall amino acid sequence identity. RUSC1/NESCA associates with TrkA, an RTK, and regulates dendritic spine dynamics by functioning as an adaptor for SNARE-mediated vesicle fusion events and as a link to molecular motor complexes (78). A role for RUSC2 in vesicular traffic has been hypothesized based on its interaction with Rab35, Rab1, and GM130 but has not been demonstrated previously (50, 52). Based on the presence of an EH domain-interacting NPF motif in RUSC2 (Fig. 7A), which is not present in RUSC1/NESCA, and the isolation of RUSC2 as part of a protein complex associated with unstimulated EGFR (53), we assessed the role of RUSC2 in EGFR trafficking. While RUSC2 did not show a physical interaction with EHD1 in cells (Fig. 7B and C), RUSC2 displayed strong colocalization with EHD1 on tubular and vesicular structures, which included the Golgi compartment (Fig. 7D and E). Importantly, RUSC2 KD led to a phenotype that

mimicked that of EHD1 KD (Fig. 8). Thus, our study provides the first direct evidence for a role of RUSC2 in anterograde EGFR trafficking out of the Golgi compartment and helps describe a novel biochemical duo of EHD1 and RUSC2 that regulates EGFR display on the cell surface. Unlike the recently described EHD1 recruitment to membranes via Rab35 effector MICAL-L1 (79), we did not find any requirement of RUSC2 for EHD1 localization in the Golgi compartment (Fig. 5B), suggesting that they function in a common trafficking pathway but independent of an interaction. In this regard, it will also be important to assess in the future if RUSC2, via its apparently functional NPF motifs, might interact with other EH domain-containing proteins to promote EGFR trafficking. The RUSC2 binding partner GM130 was recently shown to play a role in the nucleation of microtubules at the Golgi compartment through sequestration of importin-$\alpha$ and activation of the spindle assembly factor TPX2 (80). Whether EHD1- and RUSC2-dependent transport of EGFR out of the Golgi compartment might use such a microtubule network will be of considerable future interest, given the proposed role of MICAL-L1 as a link between EHD1$^+$ vesicles and dynein motors through an interaction with the collapsin response mediator protein 2 (CRMP2) at the endocytic recycling compartment (81).

Notably, several previously known EHD protein interactors have now been recognized to play a role at the Golgi compartment. For example, EHD1 interactor Rab11-FIP1/RCP was recently shown to mediate traffic at the *trans*-Golgi network through binding to golgin-97 (82). A GM130-Rab11-mediated pathway for surface expression of the T-cell antigen receptor has been described previously (83). Whether these roles involve interactions with EHD proteins will be of significant interest in future studies. Recent studies have also indicated that EHD1 depletion alters the Golgi polarization relevant to cytokinesis, while MICAL-L1 knockdown partially disrupted the Golgi reorientation toward the direction of a scratch wound (84, 85). Although we have not examined the Golgi dynamics in our studies, we did not observe any gross changes in the Golgi apparatus.

The RUSC2 gene has also been described as an HIV-1 susceptibility gene (86), and it will be of great interest in the future to assess if EHD1-RUSC2 complex plays a role in cellular pathology associated with HIV infection. EHD1 expression was recently found to be associated with poor prognosis in non-small cell lung cancer (43, 44) and breast cancer (45), and EHD1 levels in NSCLC showed a negative correlation with sensitivity to EGFR-targeted kinase inhibitor therapy (47). Thus, the new molecular pathway we identify may prove to be of clinical relevance in targeted therapy of cancers driven by aberrations of EGFR or other RTKs.

In conclusion, studies presented here demonstrate a new and functionally important role of EHD1 and a potential novel partner, RUSC2, in the control of Golgi compartment-to-surface transport of a prototype RTK, EGFR under ligand-unstimulated conditions. Using the experimental systems described here, it will be of great interest to use targeted or genome-wide knockdown/KO or ectopic gene expression approaches to identify other novel players that regulate the basal RTK surface expression and their functional roles in physiological and pathological RTK signaling.

## MATERIALS AND METHODS

**Biochemical reagents.** The reagents and their sources are as follows: puromycin, hygromycin, G418, doxycycline (Dox), enzyme immunoassay-grade bovine serum albumin (BSA), paraformaldehyde (PFA), monensin, propidium iodide, DMSO, GTP$\gamma$S (catalog number G8634), and Triton X-100 were from Sigma-Aldrich (St. Louis, MO). EGF was from PeproTech (Rocky Hill, NJ). Halt protease and phosphatase inhibitor cocktail were from Life Technologies. Normal goat serum (catalog no. 005-000-121) was from Jackson ImmunoResearch Laboratories. $^{35}$S-labeled methionine-cysteine (EXPRE$^{35}$S$^{35}$S protein labeling mix; NEG072) was from Perkin Elmer. Vectashield mounting medium was from Vector Laboratories (Burlingame, CA). NeutrAvidin Protein Dylight 488 conjugate (catalog no. 22832) was from Thermo Scientific. Glutathione-Sepharose 4B beads were from GE Healthcare. Protein G-Sepharose beads were from Invitrogen.

**Antibodies.** Anti-EGFR mouse monoclonal 528 (catalog no. Grol1) was from Calbiochem or purified from hybridoma supernatants in-house; anti-EGFR rabbit polyclonal (SC-03) and anti-HSC-70 (B-6; 7298) were from Santa Cruz Biotechnology; anti-EHD1 (ab109311) was from Abcam; anti-$\beta$-actin (A5316) was from Sigma-Aldrich; anti-Turbo-GFP (PA5-22688) was from Thermo Scientific; anti-p-Erk (9101), anti-Erk

(9102), and anti-p-EGFR (Tyr-1068;2234) were from Cell Signaling Technology; anti-GM130 (610822) was from BD Biosciences; anti-mouse IgG2a–allophycocyanin (APC) conjugate was from BioLegend (407109); and a nonspecific mouse IgG2a control (34950) was from BD Biosciences. APC–anti-human EGFR (clone Ay13; catalog no. 352906) and APC–mouse IgG2a isotype control (clone MOPC-173; 400220) were from BioLegend. Brilliant Violet 605 anti-human HLA-A, -B, -C (clone W6/32; 311432) and Brilliant Violet 605 mouse IgG2a isotype control (clone MOPC-173; 400269) were from BioLegend. In-house generated rabbit antibodies recognizing EHD1/EHD4, EHD2, EHD3 or EHD4 have been described previously (87). A rabbit polyclonal antibody against human RUSC2/iporin was generated against an internal peptide sequence (amino acid residues 532 to 553) through a commercial vendor (Pacific Immunology, Ramona, CA) and validated using epitope-tagged RUSC2 expressed in 293T cells and shRNA knockdown of endogenous RUSC2. HA tag antibody (catalog no. 901503) was from BioLegend. Anti-Myc epitope antibody (9E10; ATCC) was protein G purified in-house from hybridoma supernatants.

**Transfection reagents and plasmids.** The Dox-inducible EHD1 expression construct (pRevTRE-EHD1-GFP) was generated by cloning the full-length, PCR-amplified, human EHD1 cDNA sequences into pDest47-GFP vector in frame with GFP and subsequently subcloning the EHD1-GFP insert into pRev-Tre vector (Clontech Laboratories Inc./TaKaRa Bio) at the AgeI/ClaI sites. The PCR primers were as follows: 5′-GATCGATCaccggtTCACCATGTTCAGCTGGGTCA-3′ (forward) and 3′-GATCGATCatcgaTCATTATTTGTAG AGCTCATCCATG-5′ (reverse). The pCDNA3-based EHD1-DsRed and EHD1-myc constructs (87) and the N-terminally HA-tagged human RUSC2 construct in pSV-HA vector (50) have been described previously. Individual siRNAs or SMARTpools and Dharmafect I transfection reagent were from the Dharmacon division of ThermoFisher (Pittsburg, PA). An individual custom siRNA sequence for EHD1 (#2006) was 5′-GACAUUGGGCAUCUCUUUCUU-3′ (43). The control siRNA 5 (catalog no. D-00210-05-50), the 3′ UTR (D-019022-20), and SMARTpool (M-019022-02) siRNAs targeting EHD1 were from ThermoFisher. XtremeGENE 9 transfection reagent was from Roche Applied Science (Indianapolis, IN). siRNA transfections were performed in Opti-MEM (Life Technologies).

The following Dox-inducible lentiviral shRNA constructs were obtained from GE Healthcare: control shRNA (VSC6580), EHD1 shRNA sequence 1 (source clone, V2IHSPGG_388688; target sequence, GCTAG TTTCTGTTCTGTAA), EHD1 shRNA sequence 2 (source clone, V2IHSPGG_908952; target sequence, AAGG TCCATAAAGACTGAG); RUSC2 shRNA sequence 1 (source clone, V2IHSPGG_463376; target sequence, GCCTAGACCGAAGATCACA); RUSC2 shRNA sequence 2 (source clone, V2IHSPGG_463384; target sequence, GCTCACCAGTCATACCATG).

**Cell culture.** Media and supplements were from Life Technologies. Fetal bovine serum (FBS) and tetracycline-free FBS were from HyClone.

16A5 is an HPV16 E6/E7-immortalized derivative of the reduction-mammoplasty-derived 76N normal mammary epithelial cell (MEC) line (55) and was grown in DFCI medium containing 2 nM EGF (55) in a humidified atmosphere of 95% air and 5% $CO_2$ at 37°C. For growth factor stimulation experiments, 16A5 cells were cultured in growth factor-free D3 medium (55) for the time periods indicated in the figure legends.

Wild-type control and EHD1$^{-/-}$ mouse embryonic fibroblast (MEF) cell lines established by *in vitro* infection of NIH 3T3 protocol-immortalized *Ehd1*$^{flox/flox}$ MEFs using adeno-GFP (control) and adeno-Cre-GFP viruses, respectively, have been described previously (61). The MEFs and the triple-negative breast cancer cell line MDA-MB-231 (ATCC) were maintained in Dulbecco's modified Eagle's medium (DMEM) containing 10% FBS and supplements (88).

**Generation of 16A5 cell lines with Dox-inducible ectopic EHD1 expression or EHD1/RUSC2 knockdown.** To generate a 16A5 cell line with Dox-inducible EHD1 expression, cells were first stably transfected with pRevTet-On plasmid containing a Tet-responsive transcriptional activator (Clontech/TaKaRa) using Lipofectamine 2000 (Life Technologies), selected in medium containing 100 $\mu$g/ml G418, and individual G418-resistant, Tet-on clones were screened for inducible expression by transient transfection of pRevTRE-GFP and assessment of Dox-inducible GFP expression. A tightly inducible clone was used for stable transfection with pRevTRE-EHD1-GFP or the empty vector (pRevTRE-GFP) using Lipofectamine 2000 and selected in 50 $\mu$g/ml hygromycin, and clones were analyzed for inducible EHD1-GFP or GFP (vector only clones) after 7-day culture with 1 $\mu$g/ml Dox using Western blot analysis.

Dox-inducible lentiviral shRNA knockdown and control 16A5 cell lines (or 16A5 cells stably expressing Dox-inducible EHD1-GFP) were generated using lentiviral constructs (GE Healthcare) against EHD1 or RUSC2 (listed above). Viral transduction was performed according to the manufacturer's protocol using 14 $\mu$g/ml of Polybrene, and transductants were selected with a predetermined (2 $\mu$g/ml) concentration of puromycin for 7 days and subsequently maintained in the same concentration of puromycin.

**Quantification of cell surface EGFR and MHC-1 using FACS analysis.** 16A5 cells were seeded at $10^5$ cells per well of six-well plates (five replicates per condition) and grown in regular medium in the presence of Dox for 48 h. Cells were then either maintained in Dox-containing regular medium (steady state) or serum- and EGF-free D3 medium for 24 h, rinsed with ice-cold PBS, and released from dishes with trypsin-EDTA (Life Technologies). Trypsinization was stopped by adding trypsin inhibitor (Gibco). Cell suspensions were transferred to Eppendorf tubes and washed three times in ice-cold FACS buffer (1% bovine serum albumin in PBS) (89). Live cells were stained with APC–anti-human EGFR antibody or anti-mouse IgG2a–APC control or with Brilliant Violet 605–anti-human HLA-A, -B, and -C or Brilliant Violet 605-mouse IgG2a isotype control. FACS analyses were performed on a Becton Dickinson LSRII instrument, and data were analyzed using FlowJo software.

**Confocal immunofluorescence microscopy.** Cells were grown on coverslips, transfected where indicated, and fixed with 4% paraformaldehyde in PBS. Fixed cells were permeabilized in 0.05% Triton X-100, blocked with 10% goat serum in PBS, and incubated with primary antibodies in 1% goat

serum-PBS at 4°C overnight. After washes in PBS, the cells were incubated with the appropriate fluorochrome-conjugated secondary antibody for 1 h at room temperature. All images were acquired using a Zeiss 710 Meta confocal laser scanning microscope (Carl Zeiss) using a 40× or 63× objective with a numerical aperture of 1.0 and appropriate filters. Merged fluorescence pictures were generated and analyzed using ZEN 2012 software from Carl Zeiss.

**Western blotting.** Following cell culture and the indicated treatments, cells were rinsed twice with ice-cold PBS, and dish-attached cells were directly lysed in ice-cold Triton X-100 lysis buffer (0.5% Triton X-100, 50 mM Tris [pH 7.5], 150 mM sodium chloride) (Fisher) containing Halt EDTA-free protease inhibitor cocktail and rotated overnight. The lysates were transferred to Eppendorf tubes and spun at 13,000 rpm for 30 min at 4°C, and supernatants were collected and quantified for protein using a Pierce bicinchoninic acid (BCA) assay reagent according to the manufacturer's directions (Thermo Scientific). Forty micrograms of protein lysates was resolved by 8% sodium dodecyl sulfate-polyacrylamide gel electrophoresis (SDS-PAGE), transferred to polyvinylidene fluoride (PVDF) membrane, and immunoblotted with the indicated antibodies.

**Cell proliferation and viability assay.** A CellTiter-Glo assay was performed according to the manufacturer's specifications (Promega).

**Metabolic labeling and pulse-chase with [$^{35}$S]methionine-cysteine.** Cells pretreated with Dox were washed with and kept in methionine-cysteine-free medium (catalog no. 21013-024; Life Technologies) for 30 min and pulse-labeled with 100 $\mu$Ci of [$^{35}$S]methionine-cysteine (EXPRE$^{35}$S$^{35}$S protein labeling mix) for 20 min. The cells were then washed in medium without radioactive label and either immediately lysed (0-min chase) or incubated in regular medium with a 100-fold excess of unlabeled methionine-cysteine for a 30-, 90- or 270-min chase time before lysis. The lysates (500 $\mu$g protein) were subjected to immunoprecipitation with anti-EGFR antibody (clone 528), and the samples were resolved by SDS-PAGE. The gel was fixed, dried, and incubated with Auto-Fluor (LS-315; National Diagnostics) before drying, and signals were visualized by autoradiography. For control cells, the above-mentioned steps were the same except that the Dox pretreatment was omitted.

**FP competition assays.** All fluorescence polarization (FP) measurements were performed in 384-well, low-volume, black round-bottom polystyrene NBS microplates (Corning). Assays were set up in a total volume of 20 $\mu$l, with 1× PBS as the assay buffer. To each well, increasing concentrations (0 to 1 mM) of 10 $\mu$l of unlabeled RUSC2 peptides (amino acids 43-NPFCPPELG-51 or 101-NPFLLQEGV-109) and 10 $\mu$l of a mixture of GST-EHD1 EH domain fusion protein (at a final concentration of 15 $\mu$M) and FITC-labeled competing peptide derived from MICAL-like 1 protein (amino acids 425-NPFEEEEED-433) (at a final concentration of 100 nM) were added. The polarization values were measured at an excitation wavelength of 485 nm and emission wavelength of 538 nm using a Spectramax M5 plate reader (Molecular Devices, Sunnyvale, CA).

**GST fusion protein pulldown assays.** For glutathione *S*-transferase (GST) pulldown assays, HEK-293 cells were transiently transfected with GFP- or HA-tagged constructs in 10-cm dishes. Cells were grown for 48 h and lysed overnight at 4°C in 600 $\mu$l of lysis buffer containing 50 mM Tris (pH 7.5), 150 mM NaCl, 0.5% Triton X-100 (wt/vol), 1 mM sodium orthovanadate, 10 mM sodium fluoride, and 0.5 mM phenylmethylsulfonyl fluoride (PMSF). Cell lysate was centrifuged at 13,000 rpm to pellet the insoluble material, and protein concentration in the cleared lysate was determined using BCA reagent. One milligram of total cell lysate was incubated with 25 $\mu$g of GST fusion proteins [GST-Ctrl, GST–EHD1-(399–534), and GST–EHD1-(399–534)-W485A, representing a GST control, a GST fusion with a truncated EHD1 consisting of residues 399 to 534, and a fusion with the truncated EHD1 with a point mutation, respectively] bound to glutathione-Sepharose beads. After 3 h of incubation at 4°C, the pulldown beads were washed six times in lysis buffer (described above) and eluted in boiling sample buffer. Proteins were resolved by SDS–9% PAGE, transferred onto polyvinylidene difluoride (PVDF) membranes (IPVH00010; Millipore, Billerica, MA), and immunoblotted with anti-GFP (overnight at 4°C) or anti-HA (2 h at room temperature) antibodies. Bound antibodies were visualized using horseradish peroxidase (HRP)-conjugated protein A (10-1023; Life Technologies, Grand Island, NY) and enhanced chemiluminescence (ECL) detection (PI-32106; Thermo Scientific, Rockford, IL).

**Coimmunoprecipitation analyses.** For coimmunoprecipitation (co-IP) analyses, 1-mg aliquots of cleared lysate protein were incubated with optimized amounts of the indicated antibodies and rocked overnight at 4°C. Thirty microliters of protein G- or A-Sepharose beads (washed with PBS and blocked in 1% BSA) was added to each IP sample and rocked at 4°C for 3 h. The beads were washed six times with TX-100 lysis buffer, and bound proteins were resolved by SDS–9% PAGE, transferred to polyvinylidene difluoride (PVDF) membrane, and immunoblotted with anti-HA, anti-Myc, anti-EHD1, and anti-EGFR antibodies. Prior to washing protein G- or A-Sepharose beads, aliquots of supernatant (equal to 5% of the amount used for IP) were saved and run alongside the IP samples.

**Statistical analyses.** The results of densitometry analyses of Western blots, CellTiter-Glo assay of proliferation (as relative light units [RLU]), and flow cytometry analyses (as median mean fluorescence intensities [MFI]) were quantified and compared between groups using Student's *t* test, and data are presented as means ± standard errors of the means (SEM) of multiple experiments, with a *P* value of ≤0.05 deemed significant. Prism, version 4.0c (GraphPad), was used to perform the statistical analysis and graphical representations of the data.

## ACKNOWLEDGMENTS

We thank the Band Lab members for discussion and the staff of the University of Nebraska Medical Center (UNMC) Cell Analysis and Flow Cytometry Research Facilities for assistance.

Support was provide by the following: NIH grants CA87986 and CA105489 to H.B. and CA96844 and CA144027 to V.B.; Department of Defense grants W81XWH-17-1-0616 (H.B.) and W81XWH-07-1-0351 and W81XWH-11-1-0171 (V.B.); an NE DHHS LB506 (2018-03) grant; University of Nebraska Collaboration Initiative seed grants; pilot grants from the Fred & Pamela Buffett Cancer Center and the Pediatric Cancer Research Program at UNMC (H.B.); Institutional Development Award (IDeA) from the NIGMS of the NIH under grant number P30 GM106397; Nebraska Research Initiative Food for Health seed grant; support to UNMC core facilities from the NCI Cancer Center Support Grant (P30CA036727) to Fred & Pamela Buffett Cancer Center and the Nebraska Research Initiative; and the Raphael Bonita Memorial Fund. T.A.B., B.T.G., and L.R.C. were trainees under an NCI Cancer Biology Training Grant. I.M., N.Z., B.C.M., S.B., and P.A. received UNMC graduate assistantships. H.L. was the recipient of a China Scholarship Council graduate fellowship.

H.B. and V.B. conceived the study and secured the funding. H.B., E.C.T., I.M., B.C.M., A.M.B., N.Z., V.B., C.G., A.N., and P.K.S. designed the experiments. E.C.T., I.M., B.C.M., A.M.B., H.L., N.Z., S.C., N.I., S.B., F.M.I., P.A., T.A.B., L.R.C., B.T.G., and M.D.S. performed experiments. S.K.N. and C.G. performed bioinformatic analysis of NPF motifs. A.B. and G.Y. contributed critical reagents. E.C.T., I.M., B.C.M., H.L., C.G., S.R., A.N., and H.B. analyzed data. E.C.T., I.M., and H.B. wrote and V.B., B.C.M., N.Z., T.A.B., H.L., and L.R.C. edited the manuscript. All authors read the manuscript and provided feedback.

We declare that we have no conflicts of interest in connection with the contents of this article.

## REFERENCES

1. Regad T. 2015. Targeting RTK signaling pathways in cancer. Cancers (Basel) 7:1758–1784.
2. Sigismund S, Confalonieri S, Ciliberto A, Polo S, Scita G, Di Fiore PP. 2012. Endocytosis and signaling: cell logistics shape the eukaryotic cell plan. Physiol Rev 92:273–366. https://doi.org/10.1152/physrev.00005.2011.
3. Sorkin A, Goh LK. 2009. Endocytosis and intracellular trafficking of ErbBs. Exp Cell Res 315:683–696. https://doi.org/10.1016/j.yexcr.2008.07.029.
4. Mishra R, Hanker AB, Garrett JT. 2017. Genomic alterations of ERBB receptors in cancer: clinical implications. Oncotarget 8:114371–114392. https://doi.org/10.18632/oncotarget.22825.
5. Herbst RS. 2004. Review of epidermal growth factor receptor biology. Int J Radiat Oncol Biol Phys 59:21–26. https://doi.org/10.1016/j.ijrobp.2003.11.041.
6. Rowinsky EK. 2004. The ErbB family: targets for therapeutic development against cancer and therapeutic strategies using monoclonal antibodies and tyrosine kinase inhibitors. Annu Rev Med 55:433–457. https://doi.org/10.1146/annurev.med.55.091902.104433.
7. Gschwind A, Fischer OM, Ullrich A. 2004. The discovery of receptor tyrosine kinases: targets for cancer therapy. Nat Rev Cancer 4:361–370. https://doi.org/10.1038/nrc1360.
8. Santarius T, Shipley J, Brewer D, Stratton MR, Cooper CS. 2010. A census of amplified and overexpressed human cancer genes. Nat Rev Cancer 10:59–64. https://doi.org/10.1038/nrc2771.
9. Rakha EA, Reis-Filho JS, Ellis IO. 2008. Basal-like breast cancer: a critical review. J Clin Oncol 26:2568–2581. https://doi.org/10.1200/JCO.2007.13.1748.
10. Sigismund S, Woelk T, Puri C, Maspero E, Tacchetti C, Transidico P, Di Fiore PP, Polo S. 2005. Clathrin-independent endocytosis of ubiquitinated cargos. Proc Natl Acad Sci U S A 102:2760–2765. https://doi.org/10.1073/pnas.0409817102.
11. Roepstorff K, Grandal MV, Henriksen L, Knudsen SL, Lerdrup M, Grovdal L, Willumsen BM, van Deurs B. 2009. Differential effects of EGFR ligands on endocytic sorting of the receptor. Traffic 10:1115–1127. https://doi.org/10.1111/j.1600-0854.2009.00943.x.
12. Mosesson Y, Mills GB, Yarden Y. 2008. Derailed endocytosis: an emerging feature of cancer. Nat Rev Cancer 8:835–850. https://doi.org/10.1038/nrc2521.
13. Tomas A, Futter CE, Eden ER. 2014. EGF receptor trafficking: consequences for signaling and cancer. Trends Cell Biol 24:26–34. https://doi.org/10.1016/j.tcb.2013.11.002.
14. Chung BM, Tom E, Zutshi N, Bielecki TA, Band V, Band H. 2014. Nexus of signaling and endocytosis in oncogenesis driven by non-small cell lung cancer-associated epidermal growth factor receptor mutants. World J Clin Oncol 5:806–823. https://doi.org/10.5306/wjco.v5.i5.806.
15. Mohapatra B, Ahmad G, Nadeau S, Zutshi N, An W, Scheffe S, Dong L, Feng D, Goetz B, Arya P, Bailey TA, Palermo N, Borgstahl GE, Natarajan A, Raja SM, Naramura M, Band V, Band H. 2013. Protein tyrosine kinase regulation by ubiquitination: critical roles of Cbl-family ubiquitin ligases. Biochim Biophys Acta 1833:122–139. https://doi.org/10.1016/j.bbamcr.2012.10.010.
16. Nadeau SA, An W, Mohapatra BC, Mushtaq I, Bielecki TA, Luan H, Zutshi N, Ahmad G, Storck MD, Sanada M, Ogawa S, Band V, Band H. 2017. Structural determinants of the gain-of-function phenotype of human leukemia-associated mutant CBL oncogene. J Biol Chem 292:3666–3682. https://doi.org/10.1074/jbc.M116.772723.
17. Waterman H, Sabanai I, Geiger B, Yarden Y. 1998. Alternative intracellular routing of ErbB receptors may determine signaling potency. J Biol Chem 273:13819–13827. https://doi.org/10.1074/jbc.273.22.13819.
18. Wiley HS. 2003. Trafficking of the ErbB receptors and its influence on signaling. Exp Cell Res 284:78–88. https://doi.org/10.1016/s0014-4827(03)00002-8.
19. Herbst JJ, Opresko LK, Walsh BJ, Lauffenburger DA, Wiley HS. 1994. Regulation of postendocytic trafficking of the epidermal growth factor receptor through endosomal retention. J Biol Chem 269:12865–12873. https://doi.org/10.1074/jbc.M300477200.
20. Gomez TS, Gorman JA, de Narvajas AA, Koenig AO, Billadeau DD. 2012. Trafficking defects in WASH-knockout fibroblasts originate from collapsed endosomal and lysosomal networks. Mol Biol Cell 23:3215–3228. https://doi.org/10.1091/mbc.E12-02-0101.
21. Seaman MN, Gautreau A, Billadeau DD. 2013. Retromer-mediated endosomal protein sorting: all WASHed up! Trends Cell Biol 23:522–528. https://doi.org/10.1016/j.tcb.2013.04.010.
22. Gullapalli A, Garrett TA, Paing MM, Griffin CT, Yang Y, Trejo J. 2004. A role for sorting nexin 2 in epidermal growth factor receptor down-regulation: evidence for distinct functions of sorting nexin 1 and 2 in protein trafficking. Mol Biol Cell 15:2143–2155. https://doi.org/10.1091/mbc.e03-09-0711.
23. Caplan S, Naslavsky N, Hartnell LM, Lodge R, Polishchuk RS, Donaldson JG, Bonifacino JS. 2002. A tubular EHD1-containing compartment involved in the recycling of major histocompatibility complex class I molecules to the plasma membrane. EMBO J 21:2557–2567. https://doi.org/10.1093/emboj/21.11.2557.

24. Jovic M, Naslavsky N, Rapaport D, Horowitz M, Caplan S. 2007. EHD1 regulates β1 integrin endosomal transport: effects on focal adhesions, cell spreading and migration. J Cell Sci 120:802–814. https://doi.org/10.1242/jcs.03383.
25. Braun A, Pinyol R, Dahlhaus R, Koch D, Fonarev P, Grant BD, Kessels MM, Qualmann B. 2005. EHD proteins associate with syndapin I and II and such interactions play a crucial role in endosomal recycling. Mol Biol Cell 16:3642–3658. https://doi.org/10.1091/mbc.e05-01-0076.
26. Lin SX, Grant B, Hirsh D, Maxfield FR. 2001. Rme-1 regulates the distribution and function of the endocytic recycling compartment in mammalian cells. Nat Cell Biol 3:567–572. https://doi.org/10.1038/35078543.
27. Gokool S, Tattersall D, Seaman MN. 2007. EHD1 interacts with retromer to stabilize SNX1 tubules and facilitate endosome-to-Golgi retrieval. Traffic 8:1873–1886. https://doi.org/10.1111/j.1600-0854.2007.00652.x.
28. Naslavsky N, McKenzie J, Altan-Bonnet N, Sheff D, Caplan S. 2009. EHD3 regulates early-endosome-to-Golgi transport and preserves Golgi morphology. J Cell Sci 122:389–400. https://doi.org/10.1242/jcs.037051.
29. Valdez G, Akmentin W, Philippidou P, Kuruvilla R, Ginty DD, Halegoua S. 2005. Pincher-mediated macroendocytosis underlies retrograde signaling by neurotrophin receptors. J Neurosci 25:5236–5247. https://doi.org/10.1523/JNEUROSCI.5104-04.2005.
30. Philippidou P, Valdez G, Akmentin W, Bowers WJ, Federoff HJ, Halegoua S. 2011. Trk retrograde signaling requires persistent, Pincher-directed endosomes. Proc Natl Acad Sci U S A 108:852–857. https://doi.org/10.1073/pnas.1015981108.
31. Rotem-Yehudar R, Galperin E, Horowitz M. 2001. Association of insulin-like growth factor 1 receptor with EHD1 and SNAP29. J Biol Chem 276:33054–33060. https://doi.org/10.1074/jbc.M009913200.
32. Park SY, Ha BG, Choi GH, Ryu J, Kim B, Jung CY, Lee W. 2004. EHD2 interacts with the insulin-responsive glucose transporter (GLUT4) in rat adipocytes and may participate in insulin-induced GLUT4 recruitment. Biochemistry 43:7552–7562. https://doi.org/10.1021/bi049970f.
33. Guilherme A, Soriano NA, Furcinitti PS, Czech MP. 2004. Role of EHD1 and EHBP1 in perinuclear sorting and insulin-regulated GLUT4 recycling in 3T3-L1 adipocytes. J Biol Chem 279:40062–40075. https://doi.org/10.1074/jbc.M401918200.
34. George M, Rainey MA, Naramura M, Foster KW, Holzapfel MS, Willoughby LL, Ying G, Goswami RM, Gurumurthy CB, Band V, Satchell SC, Band H. 2011. Renal thrombotic microangiopathy in mice with combined deletion of endocytic recycling regulators EHD3 and EHD4. PLoS One 6:e17838. https://doi.org/10.1371/journal.pone.0017838.
35. Gudmundsson H, Hund TJ, Wright PJ, Kline CF, Snyder JS, Qian L, Koval OM, Cunha SR, George M, Rainey MA, Kashef FE, Dun W, Boyden PA, Anderson ME, Band H, Mohler PJ. 2010. EH domain proteins regulate cardiac membrane protein targeting. Circ Res 107:84–95. https://doi.org/10.1161/CIRCRESAHA.110.216713.
36. Gudmundsson H, Curran J, Kashef F, Snyder JS, Smith SA, Vargas-Pinto P, Bonilla IM, Weiss RM, Anderson ME, Binkley P, Felder RB, Carnes CA, Band H, Hund TJ, Mohler PJ. 2012. Differential regulation of EHD3 in human and mammalian heart failure. J Mol Cell Cardiol 52:1183–1190. https://doi.org/10.1016/j.yjmcc.2012.02.008.
37. Curran J, Makara MA, Little SC, Musa H, Liu B, Wu X, Polina I, Alecusan JS, Wright P, Li J, Billman GE, Boyden PA, Gyorke S, Band H, Hund TJ, Mohler PJ. 2014. EHD3-dependent endosome pathway regulates cardiac membrane excitability and physiology. Circ Res 115:68–78. https://doi.org/10.1161/CIRCRESAHA.115.304149.
38. Curran J, Musa H, Kline CF, Makara MA, Little SC, Higgins JD, Hund TJ, Band H, Mohler PJ. 2015. Eps15 homology domain-containing protein 3 regulates cardiac T-type $Ca^{2+}$ channel targeting and function in the atria. J Biol Chem 290:12210–12221. https://doi.org/10.1074/jbc.M115.646893.
39. Posey AD, Jr, Pytel P, Gardikiotes K, Demonbreun AR, Rainey M, George M, Band H, McNally EM. 2011. Endocytic recycling proteins EHD1 and EHD2 interact with fer-1-like-5 (Fer1L5) and mediate myoblast fusion. J Biol Chem 286:7379–7388. https://doi.org/10.1074/jbc.M110.157222.
40. Posey AD, Jr, Swanson KE, Alvarez MG, Krishnan S, Earley JU, Band H, Pytel P, McNally EM, Demonbreun AR. 2014. EHD1 mediates vesicle trafficking required for normal muscle growth and transverse tubule development. Dev Biol 387:179–190. https://doi.org/10.1016/j.ydbio.2014.01.004.
41. Cypher LR, Bielecki TA, Huang L, An W, Iseka F, Tom E, Storck MD, Hoppe AD, Band V, Band H. 2016. Corrigendum to CSF-1 receptor signalling is governed by pre-requisite EHD1 mediated receptor display on the macrophage cell surface [Cell Signalling 2016 Sep.; 28(9): 1325–35. Cell Signal 28:1933. https://doi.org/10.1016/j.cellsig.2016.07.018.
42. Chung BM, Raja SM, Clubb RJ, Tu C, George M, Band V, Band H. 2009. Aberrant trafficking of NSCLC-associated EGFR mutants through the endocytic recycling pathway promotes interaction with Src. BMC Cell Biol 10:84. https://doi.org/10.1186/1471-2121-10-84.
43. Lu H, Meng Q, Wen Y, Hu J, Zhao Y, Cai L. 2013. Increased EHD1 in non-small cell lung cancer predicts poor survival. Thorac Cancer 4:422–432. https://doi.org/10.1111/1759-7714.12043.
44. Gao Y, Wang Y, Sun L, Meng Q, Cai L, Dong X. 2014. Expression of TGFbeta-1 and EHD1 correlated with survival of non-small cell lung cancer. Tumour Biol 35:9371–9380. https://doi.org/10.1007/s13277-014-2164-x.
45. Tong D, Liang YN, Stepanova AA, Liu Y, Li X, Wang L, Zhang F, Vasilyeva NV. 2017. Increased Eps15 homology domain 1 and RAB11FIP3 expression regulate breast cancer progression via promoting epithelial growth factor receptor recycling. Tumour Biol 39:1010428317691010. https://doi.org/10.1177/1010428317691010.
46. Liu Y, Liang Y, Li M, Liu D, Tang J, Yang W, Tong D, Jin X. 2018. Eps15 homology domain 1 promotes the evolution of papillary thyroid cancer by regulating endocytotic recycling of epidermal growth factor receptor. Oncol Lett 16:4263–4270. https://doi.org/10.3892/ol.2018.9200.
47. Wang X, Yin H, Zhang H, Hu J, Lu H, Li C, Cao M, Yan S, Cai L. 2018. NF-kappaB-driven improvement of EHD1 contributes to erlotinib resistance in EGFR-mutant lung cancers. Cell Death Dis 9:418. https://doi.org/10.1038/s41419-018-0447-7.
48. Amessou M, Ebrahim AS, Dilly A, Joseph M, Tabolina M, Chukkapalli S, Meroueh L, Syed JT, Liddane A, Lang SL, Al-Katib A, Kandouz M. 2016. Spatio-temporal regulation of EGFR signaling by the Eps15 homology domain-containing protein 3 (EHD3). Oncotarget 7:79203–79216. https://doi.org/10.18632/oncotarget.13008.
49. Chukkapalli S, Amessou M, Dekhil H, Dilly AK, Liu Q, Bandyopadhyay S, Thomas RD, Bejna A, Batist G, Kandouz M. 2014. Ehd3, a regulator of vesicular trafficking, is silenced in gliomas and functions as a tumor suppressor by controlling cell cycle arrest and apoptosis. Carcinogenesis 35:877–885. https://doi.org/10.1093/carcin/bgt399.
50. Bayer M, Fischer J, Kremerskothen J, Ossendorf E, Matanis T, Konczal M, Weide T, Barnekow A. 2005. Identification and characterization of Iporin as a novel interaction partner for Rab1. BMC Cell Biol 6:15. https://doi.org/10.1186/1471-2121-6-15.
51. Chi S, Cao H, Wang Y, McNiven MA. 2011. Recycling of the epidermal growth factor receptor is mediated by a novel form of the clathrin adaptor protein Eps15. J Biol Chem 286:35196–35208. https://doi.org/10.1074/jbc.M111.247577.
52. Fukuda M, Kobayashi H, Ishibashi K, Ohbayashi N. 2011. Genome-wide investigation of the Rab binding activity of RUN domains: development of a novel tool that specifically traps GTP-Rab35. Cell Struct Funct 36:155–170. https://doi.org/10.1247/csf.11001.
53. Deribe YL, Wild P, Chandrashaker A, Curak J, Schmidt MHH, Kalaidzidis Y, Milutinovic N, Kratchmarova I, Buerkle L, Fetchko MJ, Schmidt P, Kittanakom S, Brown KR, Jurisica I, Blagoev B, Zerial M, Stagljar I, Dikic I. 2009. Regulation of epidermal growth factor receptor trafficking by lysine deacetylase HDAC6. Sci Signal 2:ra84. https://doi.org/10.1126/scisignal.2000576.
54. Goh LK, Huang F, Kim W, Gygi S, Sorkin A. 2010. Multiple mechanisms collectively regulate clathrin-mediated endocytosis of the epidermal growth factor receptor. J Cell Biol 189:871–883. https://doi.org/10.1083/jcb.201001008.
55. Band V, Sager R. 1989. Distinctive traits of normal and tumor-derived human mammary epithelial cells expressed in a medium that supports long-term growth of both cell types. Proc Natl Acad Sci U S A 86:1249–1253. https://doi.org/10.1073/pnas.86.4.1249.
56. Fukazawa T, Miyake S, Band V, Band H. 1996. Tyrosine phosphorylation of Cbl upon epidermal growth factor (EGF) stimulation and its association with EGF receptor and downstream signaling proteins. J Biol Chem 271:14554–14559. https://doi.org/10.1074/jbc.271.24.14554.
57. Duan L, Miura Y, Dimri M, Majumder B, Dodge IL, Reddi AL, Ghosh A, Fernandes N, Zhou P, Mullane-Robinson K, Rao N, Donoghue S, Rogers RA, Bowtell D, Naramura M, Gu H, Band V, Band H. 2003. Cbl-mediated ubiquitinylation is required for lysosomal sorting of epidermal growth factor receptor but is dispensable for endocytosis. J Biol Chem 278:28950–28960. https://doi.org/10.1074/jbc.M304474200.
58. Duan L, Chen G, Virmani S, Ying G, Raja SM, Chung BM, Rainey MA, Dimri M, Ortega-Cava CF, Zhao X, Clubb RJ, Tu C, Reddi AL, Naramura M, Band

V, Band H. 2010. Distinct roles for Rho versus Rac/Cdc42 GTPases downstream of Vav2 in regulating mammary epithelial acinar architecture. J Biol Chem 285:1555–1568. https://doi.org/10.1074/jbc.M109.057976.
59. Dimri M, Naramura M, Duan L, Chen J, Ortega-Cava C, Chen G, Goswami R, Fernandes N, Gao Q, Dimri GP, Band V, Band H. 2007. Modeling breast cancer-associated c-Src and EGFR overexpression in human MECs: c-Src and EGFR cooperatively promote aberrant three-dimensional acinar structure and invasive behavior. Cancer Res 67:4164–4172. https://doi.org/10.1158/0008-5472.CAN-06-2580.
60. Duan L, Raja SM, Chen G, Virmani S, Williams SH, Clubb RJ, Mukhopadhyay C, Rainey MA, Ying G, Dimri M, Chen J, Reddi AL, Naramura M, Band V, Band H. 2011. Negative regulation of EGFR-Vav2 signaling axis by Cbl ubiquitin ligase controls EGF receptor-mediated epithelial cell adherens junction dynamics and cell migration. J Biol Chem 286:620–633. https://doi.org/10.1074/jbc.M110.188086.
61. Bhattacharyya S, Rainey MA, Arya P, Mohapatra BC, Mushtaq I, Dutta S, George M, Storck MD, McComb RD, Muirhead D, Todd GL, Gould K, Datta K, Gelineau-van Waes J, Band V, Band H. 2016. Endocytic recycling protein EHD1 regulates primary cilia morphogenesis and SHH signaling during neural tube development. Sci Rep 6:20727. https://doi.org/10.1038/srep20727.
62. Alexander A. 1998. Endocytosis and intracellular sorting of receptor tyrosine kinases. Front Biosci 3:d729–d738.
63. Barzilay E, Ben-Califa N, Hirschberg K, Neumann D. 2005. Uncoupling of brefeldin a-mediated coatomer protein complex-I dissociation from Golgi redistribution. Traffic 6:794–802. https://doi.org/10.1111/j.1600-0854.2005.00317.x.
64. Johns TG, Mellman I, Cartwright GA, Ritter G, Old LJ, Burgess AW, Scott AM. 2005. The antitumor monoclonal antibody 806 recognizes a high-mannose form of the EGF receptor that reaches the cell surface when cells over-express the receptor. FASEB J 19:780–782. https://doi.org/10.1096/fj.04-1766fje.
65. Franovic A, Gunaratnam L, Smith K, Robert I, Patten D, Lee S. 2007. Translational up-regulation of the EGFR by tumor hypoxia provides a nonmutational explanation for its overexpression in human cancer. Proc Natl Acad Sci U S A 104:13092–13097. https://doi.org/10.1073/pnas.0702387104.
66. Gamou S, Shimizu N. 1987. Change in metabolic turnover is an alternate mechanism increasing cell surface epidermal growth factor receptor levels in tumor cells. J Biol Chem 262:6708–6713.
67. Wang YN, Wang H, Yamaguchi H, Lee HJ, Lee HH, Hung MC. 2010. COPI-mediated retrograde trafficking from the Golgi to the ER regulates EGFR nuclear transport. Biochem Biophys Res Commun 399:498–504. https://doi.org/10.1016/j.bbrc.2010.07.096.
68. Calhoun BC, Goldenring JR. 1996. Rab proteins in gastric parietal cells: evidence for the membrane recycling hypothesis. Yale J Biol Med 69:1–8.
69. Allan BB, Moyer BD, Balch WE. 2000. Rab1 recruitment of p115 into a cis-SNARE complex: programming budding COPII vesicles for fusion. Science 289:444–448. https://doi.org/10.1126/science.289.5478.444.
70. Mukhopadhyay A, Quiroz JA, Wolkoff AW. 2014. Rab1a regulates sorting of early endocytic vesicles. Am J Physiol Gastrointest Liver Physiol 306:G412–G424. https://doi.org/10.1152/ajpgi.00118.2013.
71. Hynes NE, Lane HA. 2005. ERBB receptors and cancer: the complexity of targeted inhibitors. Nat Rev Cancer 5:341–354. https://doi.org/10.1038/nrc1609.
72. Naslavsky N, Caplan S. 2011. EHD proteins: key conductors of endocytic transport. Trends Cell Biol 21:122–131. https://doi.org/10.1016/j.tcb.2010.10.003.
73. Zhang J, Reiling C, Reinecke JB, Prislan I, Marky LA, Sorgen PL, Naslavsky N, Caplan S. 2012. Rabankyrin-5 interacts with EHD1 and Vps26 to regulate endocytic trafficking and retromer function. Traffic 13:745–757. https://doi.org/10.1111/j.1600-0854.2012.01334.x.
74. McKenzie JE, Raisley B, Zhou X, Naslavsky N, Taguchi T, Caplan S, Sheff D. 2012. Retromer guides STxB and CD8-M6PR from early to recycling endosomes, EHD1 guides STxB from recycling endosome to Golgi. Traffic 13:1140–1159. https://doi.org/10.1111/j.1600-0854.2012.01374.x.
75. Scott CC, Vacca F, Gruenberg J. 2014. Endosome maturation, transport and functions. Semin Cell Dev Biol 31:2–10. https://doi.org/10.1016/j.semcdb.2014.03.034.
76. Iseka FM, Goetz BT, Mushtaq I, An W, Cypher LR, Bielecki TA, Tom EC, Arya P, Bhattacharyya S, Storck MD, Semerad CL, Talmadge JE, Mosley RL, Band V, Band H. 2018. Role of the EHD family of endocytic recycling regulators for TCR recycling and T cell function. J Immunol 200:483–499. https://doi.org/10.4049/jimmunol.1601793.
77. Sengupta S, George M, Miller KK, Naik K, Chou J, Cheatham MA, Dallos P, Naramura M, Band H, Zheng J. 2009. EHD4 and CDH23 are interacting partners in cochlear hair cells. J Biol Chem 284:20121–20129. https://doi.org/10.1074/jbc.M109.025668.
78. MacDonald JI, Dietrich A, Gamble S, Hryciw T, Grant RI, Meakin SO. 2012. Nesca, a novel neuronal adapter protein, links the molecular motor kinesin with the pre-synaptic membrane protein, syntaxin-1, in hippocampal neurons. J Neurochem 121:861–880. https://doi.org/10.1111/j.1471-4159.2012.07729.x.
79. Sharma M, Giridharan SS, Rahajeng J, Naslavsky N, Caplan S. 2009. MICAL-L1 links EHD1 to tubular recycling endosomes and regulates receptor recycling. Mol Biol Cell 20:5181–5194. https://doi.org/10.1091/mbc.e09-06-0535.
80. Wei JH, Zhang ZC, Wynn RM, Seemann J. 2015. GM130 regulates Golgi-derived spindle assembly by activating TPX2 and capturing microtubules. Cell 162:287–299. https://doi.org/10.1016/j.cell.2015.06.014.
81. Rahajeng J, Caplan S, Naslavsky N. 2010. Common and distinct roles for the binding partners Rabenosyn-5 and Vps45 in the regulation of endocytic trafficking in mammalian cells. Exp Cell Res 316:859–874. https://doi.org/10.1016/j.yexcr.2009.11.007.
82. Jing J, Junutula JR, Wu C, Burden J, Matern H, Peden AA, Prekeris R. 2010. FIP1/RCP binding to Golgin-97 regulates retrograde transport from recycling endosomes to the trans-Golgi network. Mol Biol Cell 21:3041–3053. https://doi.org/10.1091/mbc.E10-04-0313.
83. Onnis A, Finetti F, Patrussi L, Gottardo M, Cassioli C, Spano S, Baldari CT. 2015. The small GTPase Rab29 is a common regulator of immune synapse assembly and ciliogenesis. Cell Death Differ 22:1687–1699. https://doi.org/10.1038/cdd.2015.17.
84. Reinecke JB, Katafiasz D, Naslavsky N, Caplan S. 2015. Novel functions for the endocytic regulatory proteins MICAL-L1 and EHD1 in mitosis. Traffic 16:48–67. https://doi.org/10.1111/tra.12234.
85. Reinecke JB, Katafiasz D, Naslavsky N, Caplan S. 2014. Regulation of Src trafficking and activation by the endocytic regulatory proteins MICAL-L1 and EHD1. J Cell Sci 127:1684–1698. https://doi.org/10.1242/jcs.133892.
86. Brass AL, Dykxhoorn DM, Benita Y, Yan N, Engelman A, Xavier RJ, Lieberman J, Elledge SJ. 2008. Identification of host proteins required for HIV infection through a functional genomic screen. Science 319:921–926. https://doi.org/10.1126/science.1152725.
87. George M, Ying G, Rainey MA, Solomon A, Parikh PT, Gao Q, Band V, Band H. 2007. Shared as well as distinct roles of EHD proteins revealed by biochemical and functional comparisons in mammalian cells and C. elegans. BMC Cell Biol 8:3. 2121–8-3. https://doi.org/10.1186/1471-2121-8-3.
88. Zhao X, Goswami M, Pokhriyal N, Ma H, Du H, Yao J, Victor TA, Polyak K, Sturgis CD, Band H, Band V. 2008. Cyclooxygenase-2 expression during immortalization and breast cancer progression. Cancer Res 68:467–475. https://doi.org/10.1158/0008-5472.CAN-07-0782.
89. Ahmad G, Mohapatra BC, Schulte NA, Nadeau SA, Luan H, Zutshi N, Tom E, Ortega-Cava C, Tu C, Sanada M, Ogawa S, Toews ML, Band V, Band H. 2014. Cbl-family ubiquitin ligases and their recruitment of CIN85 are largely dispensable for epidermal growth factor receptor endocytosis. Int J Biochem Cell Biol 57:123–134. https://doi.org/10.1016/j.biocel.2014.10.019.